Tectonics

RESEARCH ARTICLE
10.1029/2018TC005300

Triassic Sedimentary Filling and Closure of the Eastern Paleo-Tethys Ocean: New Insights From Detrital Zircon Geochronology of Songpan-Ganzi, Yidun, and West Qinling Flysch in Eastern Tibet

Xing Jian[1], **Amy Weislogel**[2], **and Alex Pullen**[3]

[1]State Key Laboratory of Marine Environmental Science, College of Ocean and Earth Sciences, Xiamen University, Xiamen, China, [2]Geology and Geography, West Virginia University, Morgantown, WV, USA, [3]Department of Environmental Engineering and Earth Sciences, Clemson University, Clemson, SC, USA

Abstract Triassic flysch in the Songpan-Ganzi Complex (SGC), eastern Tibet, is an important and rich record of tectonism associated with evolution and closure of the eastern Paleo-Tethys Ocean. However, current models for tectonic evolution of the ocean remain controversial, in large part due to ambiguity of the origin of SGC deposits. We constrain provenance of Middle-Upper Triassic turbidites from central SGC and the adjacent Yidun and West Qinling terranes by using detrital zircon U-Pb geochronology. The results show that the detrital zircon ages mainly comprise five populations: 240–310 Ma; 400–480 Ma; 750–1,000 Ma; 1,700–2,000 Ma; and 2,300–2,600 Ma. These ages indicate the East Kunlun and North China block served as major sediment sources for most of central SGC and West Qinling. The predominance of Paleozoic zircons in Upper Triassic turbidites indicates uplift and exhumation of the East Kunlun orogen during the Late Triassic. The southern SGC and Yidun turbidites display quite similar zircon age spectra (significant age peaks at approximately 1,850 Ma), implying that Songpan-Ganzi and Yidun depocenters were adjacent to each other by the Middle Triassic. This finding suggests that the Ganzi-Litang Ocean, as a part of eastern Paleo-Tethys Ocean, probably had been closed by the Middle Triassic. We favor subsequent deformation and uplift of the Triassic flysch was coeval with or possibly predated latest Triassic shortening within the Longmenshan thrust belt, resulting in recycling of the flysch into surrounding sedimentary basins (e.g., Sichuan and Qamdo basins) since latest Triassic time.

Key Points:
- Amalgamation of the Songpan-Ganzi Complex and Yidun terrane, and closure of the Ganzi-Litang Ocean, had occurred by the Middle Triassic
- The East Kunlun, on northern margin of the eastern Paleo-Tethys, underwent significant exhumation and erosion during the Late Triassic
- Deformation of the Songpan-Ganzi and Yidun flysch strata was coeval with or predated latest Triassic shortening within Longmenshan

Supporting Information:
- Supporting Information S1
- Data Set S1

Correspondence to:
X. Jian,
xjian@xmu.edu.cn

Citation:
Jian, X., Weislogel, A., & Pullen, A. (2019). Triassic sedimentary filling and closure of the eastern Paleo-Tethys Ocean: New insights from detrital zircon geochronology of Songpan-Ganzi, Yidun, and West Qinling flysch in eastern Tibet. *Tectonics*, *38*. https://doi.org/10.1029/2018TC005300

Received 24 AUG 2018
Accepted 31 JAN 2019
Accepted article online 4 FEB 2019

1. Introduction

The Songpan-Ganzi Complex (SGC), located in the eastern Tibetan Plateau, is a triangular expanse of intensely deformed Middle-Upper Triassic (Anisian through Norian; Nie et al., 1994) flysch wedged amid a complicated collage of tectonic blocks and orogenic belts. The SGC is characterized by thick (averaging approximately 8 km) and widespread (>300,000 km^2) deep-water marine calciclastic and siliciclastic gravity massive flow deposits identified as the largest Triassic accumulation of sediment on Earth and one of the largest sinks by volume of submarine clastic detritus preserved over geologic time scales (Chang, 2000; Nie et al., 1994; Xu et al., 1992). As such, it has attracted considerable attention and study for decades (e.g., Billerot et al., 2017; Chang, 2000; de Sigoyer et al., 2014; Ding et al., 2013; Nie et al., 1994; Roger et al., 2004, 2010; She et al., 2006; Weislogel et al., 2006, 2010; Zhang et al., 2008).

Development of the Songpan-Ganzi basin (SGB) during the Middle-Late Triassic and subsequent deformation occurred synchronously with several significant geological events in this region, including (1) collision between the North China block (NCB) and South China block (SCB) and ultrahigh-pressure metamorphism of the Dabie terrane (Faure et al., 2001; Hacker et al., 2004; Meng & Zhang, 2000; Yin & Nie, 1993), (2) closure of the eastern Paleo-Tethys Ocean (PTO; Liu et al., 2015), (3) plate convergence and collision along major suture zones (Pullen et al., 2008; Roger et al., 2003, 2010; Yang et al., 2012, 2014; Zhang et al., 2006), and (4) thrust faulting in the Longmenshan thrust belt and exhumation of eastern Tibet (Burchfiel et al., 1995; Harrowfield & Wilson, 2005; Huang et al., 2003; Worley & Wilson, 1996; Yong et al., 2003). Triassic clastic sediment influx into the basin thus preserves records of tectonic evolution for both the sediment source areas and the eastern PTO, which hosted the SGC itself. However, the provenance of SGC deposits remains ambiguous in part due to a lack of clear correlation of the flysch strata with preserved

deposits of one or more associated terrestrial feeder depositional systems. In addition, identification of sediment transport systems is hindered by structural overprinting from subsequent tectonism and deformation associated with ocean basin closure.

Previous detrital zircon provenance studies on the SGC flysch have generated a variety of interpretations about the associated source areas and by association the tectonic setting of the basin. Investigations on the eastern SGC turbidites (e.g., Brugier et al., 1997; Weislogel et al., 2006, 2010) suggested that collisional orogenic belts between NCB and SCB, including the southern margin of the NCB and the northern margin of the SCB, were the major sediment source areas. This led to the interpretation of the eastern PTO as a remnant ocean basin, in which flysch deposition was analogous to the Cenozoic Bengal fan (Copeland & Harrison, 1990). Alternate interpretations for SGC turbidite provenance and tectonic setting have been developed based on a regional data set of detrital zircon ages from across the entire SGC, including the Hol-Xil area in the western area of the SGC (Figure 1). Ding et al. (2013) contended that the Neoproterozoic zircons found in these turbidites were preferred to be derived from the western margin of the SCB. And the SCB detritus was proposed to be transported into the eastern PTO by large-scale (>1500 km) horizontal transport systems that infilled the eastern PTO as back-arc extension from slab roll-back rifted the Yidun terrane away from the West Qinling/East Kunlun, consistent with the Mediterranean-style model proposed by Pullen et al. (2008). However, Ding et al. (2013) noted that the transport of SCB-derived material into the Hoh-Xil region required rapid progradation of submarine fans (>150 km/Ma) or else these sediments were sourced from unrecognized material near the Hoh-Xil region with a detrital zircon signature similar to the SCB. Also, Y. X. Zhang et al. (2014) added detrital zircon ages from five turbidite samples and advocated that the Kunlun and Qinling orogens mainly supplied sediment to the northern SGC, along with some amount of sediment contribution from the Qiangtang terrane, which has crust of Gondwanan origin and could have supplied zircons of *Pan-African* age (500–650 Ma).

These existing models of the SGB development imply significant differences in tectonic setting and basin evolution for the eastern PTO. The discrepancy among models is in large part due to the poorly characterized provenance record for the central SGC deposits. The paleogeographic position of the central SGC lies at the juncture of several potential source areas, such as NCB, SCB, East Kunlun, Qinling-Dabie, and Qiangtang terrane, which would impart variable provenance signatures on SGC detritus. Thus, the Triassic sedimentary record of the central SGC could be used to reconstruct crucial paleogeographic relationships and to test the existing models of early Mesozoic tectonic evolution for the eastern PTO.

Here we present provenance analysis results for Middle-Upper Triassic turbidites from central SGC, Yidun, and West Qinling terranes, based on paleocurrent orientations, sandstone framework-grain petrography, and detrital zircon U-Pb geochronology. Our sampling targeted regions where SGC provenance has been poorly characterized and included sampling basement rocks from the East Kunlun orogen, Zhongza massif, and the Longmenshan thrust belt for comparison (Figure 1). From spatial and temporal variation of detrital zircon age distributions of SGC, Yidun, and West Qinling turbidites and through comparison with detrital zircon ages from basement rocks, we interpret the provenance and filling history of the eastern PTO and reconstruct the Triassic tectonic evolution of SGC and adjacent regions in the eastern Tibetan Plateau.

2. Geological Setting

2.1. SGC

The SGC flysch deposits are currently folded and sit at elevations of ~4,000 m forming a major lithospheric terrane of eastern Tibet, spanning ~2,000 km from east to west and as much as 500 km from north to south in present coordinates. The SGC is bound by the Kunlun-Qaidam-Qilian-Qinling terranes and NCB to the north, the Qiangtang and Yidun terranes to the south, and the Longmenshan thrust belt and SCB to the east (Figure 1; Nie et al., 1994; Xu et al., 1992; Yin & Harrison, 2000). The SGB represents a remnant of eastern PTO, which occupied the area between Eurasia and Gondwana from late Paleozoic to early Mesozoic (Metcalfe, 2006). Northward subduction of Paleo-Tethyan oceanic lithosphere beneath the amalgamated North China-Kunlun-Qaidam continental lithosphere started in the Late Devonian or Early Permian (Matte et al., 1996). The elongated Cimmerian plate, including the Qiangtang terrane, rifted from Gondwana by the Late Permian and began moving northward (Gehrels et al., 2011; Pullen & Kapp, 2014); by the latest Triassic, the Yidun terrane, possibly joined with the Qiangtang terrane to its west along the

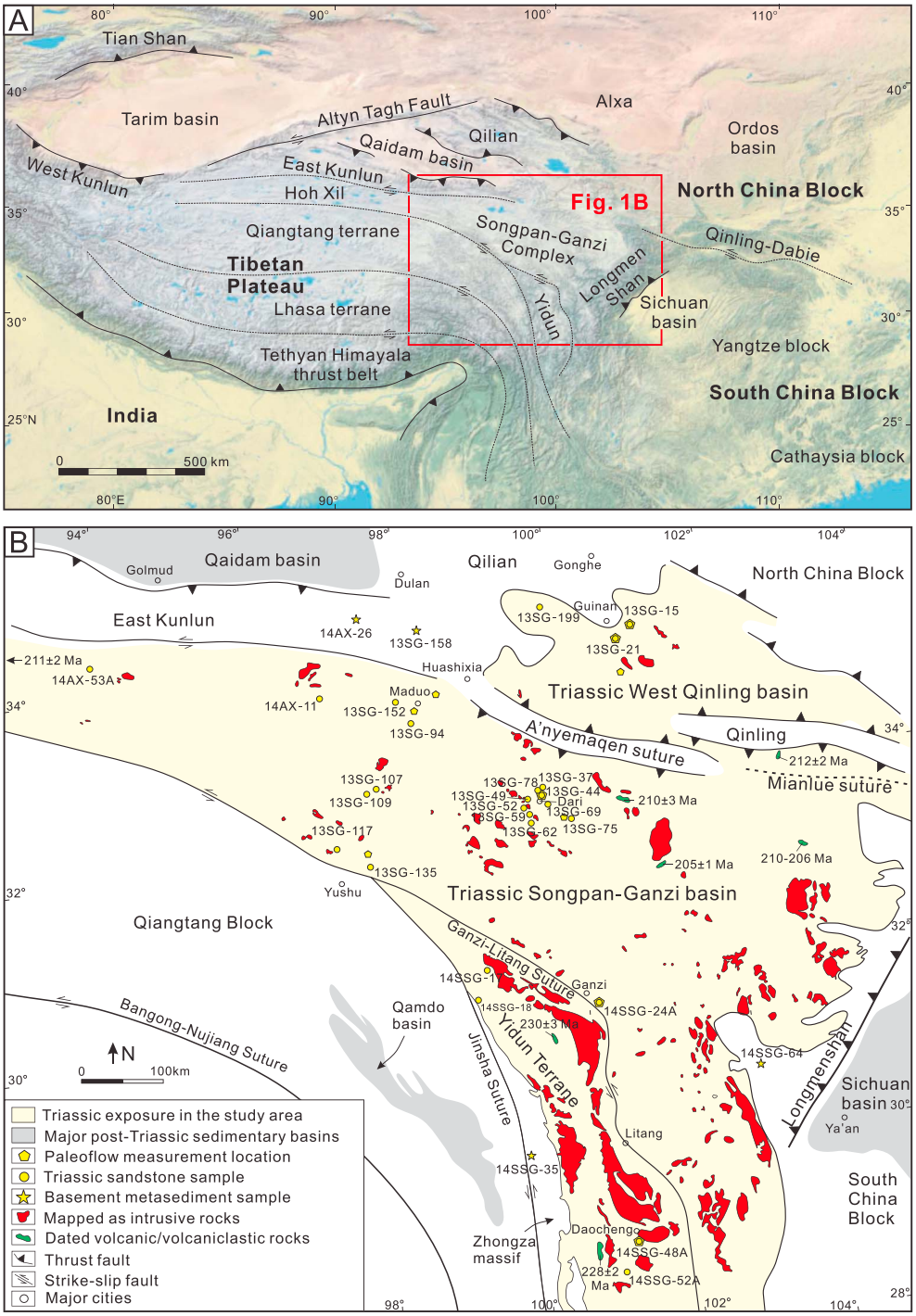

Figure 1. (a) Tectonic location of the Songpan-Ganzi Complex in eastern Tibet. (b) Geological setting of the West Qinling, central Songpan-Ganzi Complex and Yidun terrane, modified from Yan et al. (2014). The paleocurrent measuring and sampling locations are marked as yellow-filled pentagons and circles, respectively. The zircon U-Pb age data of volcanic/volcaniclastic rock interbeds in the turbidites are from Cai et al. (2010), Wang et al. (2011), Wang, Zhou, et al. (2013), and Li et al. (2016).

Jinsha suture (Yang et al., 2012, 2014; Zi et al., 2012), converged upon the SGC due to subduction along the Ganzi-Litang suture (Figure 1b; Hou, 1993; Wu et al., 2016). Late-stage evolution and closure of the eastern PTO are recorded by substantial shortening and low-grade greenschist facies metamorphism of SGC flysch strata (Chang, 2000; Huang et al., 2003; Roger et al., 2010). The SGB was extensively intruded by Late

Triassic-Early Jurassic igneous rocks, mainly A-type, I-type, and adakitic granitoids (L. Y. Zhang et al., 2014, and references therein). Previous studies provided different interpretations for the origins of the magmatism, including partial melting of thickened lower continental crust and/or Paleo-Tethys subducted oceanic slab (adakitic rocks), postcollisional settings (A-type), and partial melting of lithospheric mantle (e.g., de Sigoyer et al., 2014; Lu et al., 2017; Yuan et al., 2010; L. Y. Zhang et al., 2014).

2.2. Yidun Terrane

The Yidun terrane, which is bounded by the Jinsha and Ganzi-Litang sutures, is located to the southwest of the SGC (Figure 1). From west to east, it includes the Precambrian-Paleozoic Zhongza massif, Middle Triassic-Early Jurassic eastern Yidun felsic plutons, and middle Cretaceous West Yidun felsic plutons (Figure 1b). The Zhongza massif is composed of Neoproterozoic basement rocks consisting of granitic gneisses and metavolcanic rocks (Bureau of Geology and Mineral Resources of Sichuan Province [BGMRSP], 1991) and a cover sequence of Paleozoic greenschist facies metasedimentary rocks, shallow- to deep-marine carbonates, and clastic rocks intercalated with sporadic mafic volcanic rocks (BGMRSP, 1991; Chang, 2000). The Zhongza massif has previously been interpreted as a microcontinent that rifted from the western Yangtze block during the opening of the Ganzi-Litang Ocean in the Late Permian (Hou, 1993; Song et al., 2004). The eastern Yidun Terrane includes widespread exposure of the Triassic Yidun Group flysch that is intruded by large Late Triassic dioritic-granitic plutons (Jackson et al., 2018a, 2018b; Reid et al., 2007; Weislogel, 2008). Similar to the Late Triassic granitoids intruded into the SGB flysch, the origin of the Yidun felsic intrusive rocks is widely debated, but most models invoke partial melting of thickened lithosphere or lower crust (e.g., Hou, 1993; Peng et al., 2014; Roger et al., 2010; Yuan et al., 2010).

2.3. West Qinling Terrane

The West Qinling is a part of Kunlun-Qilian-Qinling central orogenic belt of China and currently borders with the Mesozoic SGC by the A'nyemaqin ophiolite mélange zone and the Mianlue suture (Figure 1). The West Qinling, as well as the surrounding Kunlun-Qilian-Qaidam terranes, accreted to the NCB prior to the Late Permian (Yin & Harrison, 2000). The A'nyemaqin suture, connecting with the Qinling-Dabie orogen (i.e., the Mianlue suture) to the east and the Kunlun suture to the west, is widely thought to have also accommodated the subduction of the PTO (Bian et al., 2004; Guo et al., 2007; Meng & Zhang, 2000; Yang et al., 1996). Middle-Late Triassic deep-water marine deposits are also widely distributed in the West Qinling area (Meng et al., 2007), but the relationship between Triassic Songpan-Ganzi and West Qinling basins is still poorly known. Proposed tectonic models for the Triassic West Qinling include an intercontinental trumpet-like rift with a westward opening between NCB and SCB (Yin et al., 1992), a forearc basin overlying a late Paleozoic ophiolitic complex (Yan et al., 2014), a back-arc basin separated from the main Songpan-Ganzi remnant ocean by the Kunlun arc (Yin & Harrison, 2000) and belonging to the northeastern part of the SGB (Li et al., 2014; Weislogel et al., 2010; Zhou & Graham, 1996).

2.4. Triassic Stratigraphic Frameworks of the Central SGC, Yidun, and West Qinling Terranes

Triassic strata in the central SGC are named the Bayan Har Group (Table 1) and include calciclastic and siliciclastic turbidites in the Lower and Middle Formations, while the Upper Formation comprises siliciclastic-dominated turbidites (BGMRQP, 1991). The depositional ages of the Bayan Har Group succession can be well constrained in the Triassic, by the youngest detrital zircon ages (265–211 Ma; Ding et al., 2013, and this study), approximately 211–205-Ma volcanic rock interbeds (Figure 1b; Cai et al., 2010; Wang et al., 2011), and widespread Norian (Late Triassic) intrusive rocks (L. Y. Zhang et al., 2014, and references therein). This is consistent with the Late Triassic ages of volcanic/volcaniclastic rock interlayers (212–205 Ma) in the eastern SGC turbidites (Figure 1b; Li et al., 2016). Triassic strata in the Yidun terrane, named as Yidun Group, include five stratigraphic units, in order from oldest to youngest: Dangen, Lieyi, Qugasi, Tumugou, and Lanashan Formations (Table 1). Volcanic rocks intercalated with turbidites of the Qugas and Tumugou Formations were dated as approximately 230–228 Ma (Wang, Zhou, et al., 2013). Geological mapping results of the West Qinling area indicate that the Lower and Middle Triassic, including the Longwuhe and Gulangdi Formations (Table 1), are composed of carbonate and siliciclastic gravity massive flow sediments, whereas the Upper Triassic, that is, the Duofutun Group, consists of continental felsic volcanoclastic rocks (BGMRQP, 1991; Meng et al., 2007). For the details of biostratigraphic constrains and

Tectonics

10.1029/2018TC005300

Table 1
Triassic Stratigraphy of the Central Songpan-Ganzi Complex, Yidun, and West Qinling Terranes

Epoch	West Qinling terrane			Central Songpan-Ganzi Complex			Yidun Terrane		
Late Triassic	Duofutun Group	Huari Fm.	Continental intermediate-acid volcanoclastic rocks	Non-deposition					
		Rinaore Fm.		Bayan Har Group	Upper Fm.	Thick gray and yellowish-brown sandstones and black mudstones. Finer sandstones and more mudstones present in western and southern area. *Halobia* sp., *H.* cf. *cordillerana*, *H.* cf. *pluriradiata*, and *H.* cf. *superbescens*.	Yidun Group	Lanashan Fm.	Dark grey slates with sandstone interbeds. *Burmesia lirata*.
								Tumugou Fm.	Grey slates and limestone with sandstone interbedds, intermediate-felsic volcanic rocks. *Cladiscites* sp.
Middle Triassic	Gulangdi Fm.		Fine sandstones, limestones and mudstones, and occasional coarser clastic sediments in the upper parts. Lenotropites sp., Leiophyllites sp., Sturia sp. Prochadiscites sp.		Middle Fm.	Thin sandstone and mudstone layers with limestones and marls in the lower parts. *Lenotropites* sp., *Danubites* sp., and *Tusuohuthyris sulcus*.		Qugasi Fm.	Dark grey carbonaceous slates and grey slates with sandstone interbedds, local mafic volcanic rocks. *Proarcestes gaytani*.
								Lieyi Fm.	Blcok carbonaceous slates, grey sandstone with interlayered pelitic siltstones. *Daonella indica*, *Halobia rugosoides*.
Early Triassic	Longwuhe Fm.		Sandstones, siltstones and mudstones with subordinate limestones, marls and conglomerates. *Claraia* cf. *stachei*, C. cf. *griesbachi*, C. cf. *delongensis*.		Lower Fm.	Interbedded sandstones and mudstones with subordinate limestones and marls. The southern area is lack of this unit. *Nevitaria* sp., *Vishnuties* sp., and *Posidonia* sp.		Dangen Fm.	Dark grey siltstones, sandstones and slates with interlayered limestones. *Claraia* cf. *stachei*, C. cf. *griesbachi*.

Note. BGMRQP (1991), BGMRSP (1991), and Meng et al. (2007).

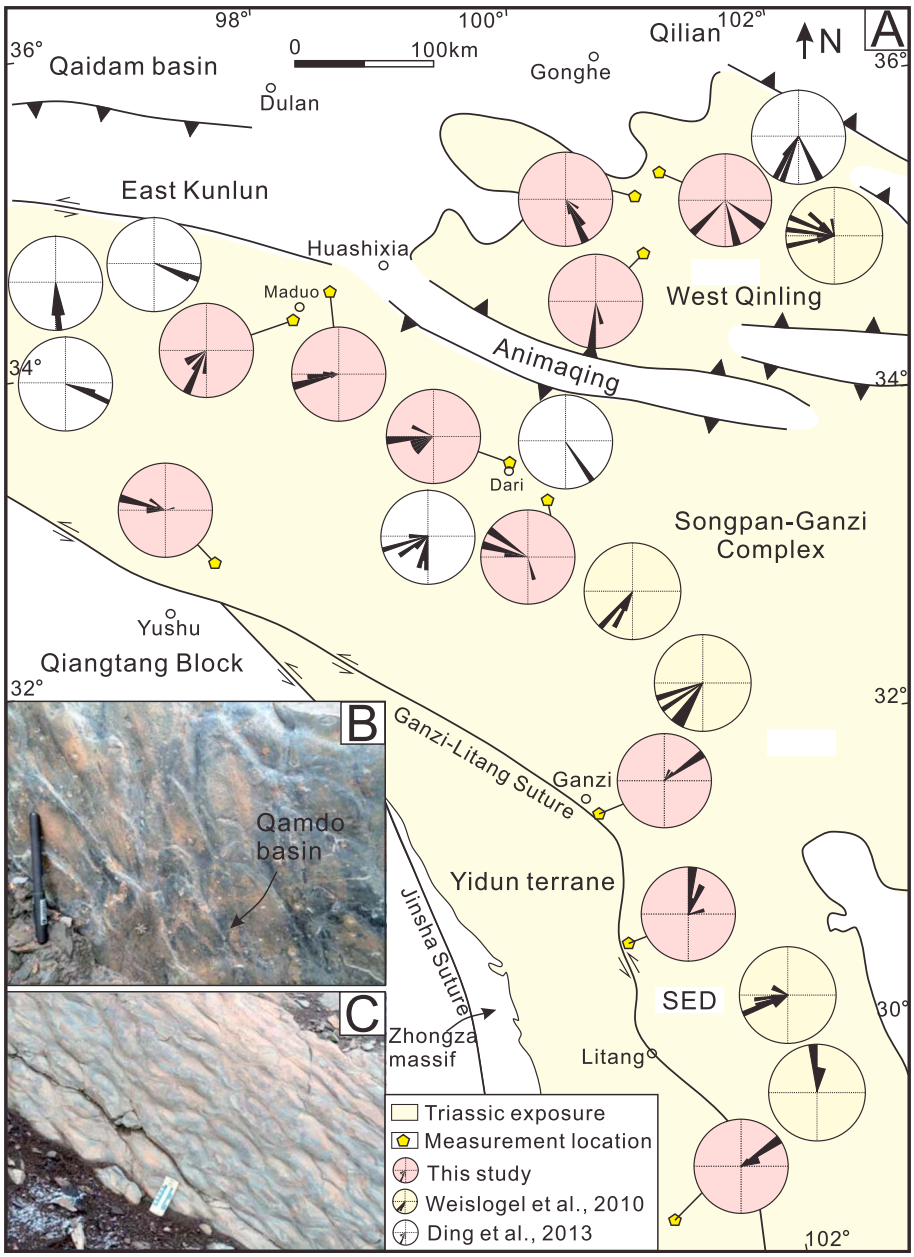

Figure 2. (a) Paleocurrent orientations measured in this study (pink) and previous studies (white and light yellow). The measurement in this study was based on (b) flute casts, (c) ripple foresets, and gravel imbrications.

lithostratigraphical descriptions of the Triassic central SCG, Yidun and West Qinling terranes, refer to BGMRQP (1991), BGMRSP (1991), and Wang, Wang, et al. (2013).

3. Sampling and Analytical Methods

Turbidite samples were collected from 94 outcrops and primarily include Middle-Upper Triassic fine- to medium-grained (meta-) sandstones. Precambrian and Paleozoic metasedimentary rock samples were collected from 12 outcrops of the potential source areas, including the East Kunlun orogen, Zhongza massif, and Longmenshan thrust belt. Each sample consisted of 2- to 3-kg fresh rocks. Paleocurrent orientation data were collected from 11 locations in our study area (Figure 2). These locations include some sampled outcrops and other outcrops where such indicators were accessible (Figures 1 and 2). The paleocurrent orientations

were mainly determined by flute casts, ripple foresets, and gravel imbrications (Figures 2b and 2c). Measurements were corrected for horizontal bedding rotations. Deformation of the Triassic turbidite strata is characterized by long cylindrical folds (BGMRSP, 1991); complex stratigraphic deformations, such as plunging folds and superposed folds, were avoided in paleocurrent data collection. Although the SGC strata were intensely folded, paleomagnetic studies indicate negligible vertical axis rotations in the majority of the northern Tibetan Plateau (e.g., Cogné et al., 1999; Dupont-Nivet et al., 2002; Halim et al., 1998). This is also reinforced by global positioning system measurements (Chen et al., 2000; Royden et al., 1997), which suggest that modern clockwise rotation, driven by convergence of India and Eurasia, mainly affects the region southwest of the Xianshuihe fault, with minimal rotation in the areas to the north.

Petrographic observations and modal analysis were carried out on 16 selected sample thin sections, using the Gazzi-Dickinson method (Dickinson, 1985; Jian et al., 2013), with 300–500 points counted per sample (Table S1 in the Data Set S1).

Twenty-nine samples were selected for detrital zircon U-Pb analysis (Table S2 in the Data Set S1). In preparation for isotopic analysis, zircons were imaged using electron backscatter detection. Laser ablation multicollector inductively coupled plasma mass spectrometer U-Th-Pb analysis of a random selection of detrital zircon cores was conducted on a Nu Plasma HR multicollector inductively coupled plasma mass spectrometer coupled to a Photon Machines 193-nm excimer laser with a approximately 30-μm spot size in the University of Arizona LaserChron center (Gehrels et al., 2008). At least 100 grains were analyzed each detrital sample. Interelemental and mass fractionation, along with session-wide instrumental drift, was corrected using standard-sample bracketing with the Sri Lanka and R33 zircon reference materials. The correction for initial-Pb on $^{206}Pb/^{238}U$ and $^{206}Pb/^{207}Pb$ was based on ^{204}Hg-corrected measured ^{204}Pb. Raw data were reduced using NUPMagecalc (Gehrels et al., 2008). Results were analyzed and plotted using Isoplot 3.0 (Ludwig, 2012) and DensityPlotter (Vermeesch, 2012). Following the conventional reporting of detrital zircon dates, the dates with poor precision (> ±10%), high discordance (> ±20%), or reverse discordance (> ±5%) were omitted from the probability density function, the kernel density estimation plots, and from interpretation. Ages <900 Ma are based on initial-Pb corrected $^{206}Pb/^{238}U$ ratios, whereas ages >900 Ma are based on initial-Pb corrected $^{206}Pb/^{207}Pb$ ratios.

4. Results

4.1. Paleocurrent Measurement

Paleocurrent orientations in the West Qinling area trend toward the south and southeast, whereas paleocurrent orientations in the central SGC indicate dominantly southwest and west directed paleoflow (Figure 2). In the southern SGC and the Yidun terrane, north and northeast directed paleoflow orientations prevail (Figure 2). These paleocurrent measurements are consistent with previous paleoflow studies (Ding et al., 2013; Weislogel et al., 2010).

4.2. Triassic Turbidite Detrital Framework Petrology and Modal Analysis

Detrital framework grains of most Triassic turbidite sandstone samples range from 700 to 100 μm. They are angular to subangular and poorly to moderately sorted (Figure S1). These sandstones contain abundant quartz, sedimentary lithic fragments, and meta-sedimentary lithic fragments. The average quartz-feldspar-lithic fragment (Q-F-L) ratios of Middle Triassic and Upper Triassic samples are 60:17:23 and 60:14:26, respectively. Modal data plotted on the Q-F-L provenance discrimination ternary diagram (Figure S1) indicate the SGC turbidite sandstone samples originated from a recycled orogenic source, and on Qp-Lvm-Lsm provenance discrimination diagrams (Figure S1), the results further indicate derivation from a collision suture and fold-thrust belt source (Dickinson, 1985). Furthermore, some sandstones show that they experienced some low-grade metamorphism, especially for the turbidites from the southern SGC and Yidun terrane. The point-count data of analyzed sandstone thin sections are presented in Table S1.

4.3. Triassic Turbidite Detrital Zircon U-Pb Geochronology

We report a total of 2,558 detrital zircon U-Pb ages from 25 Triassic turbidite samples, including 15 samples from the central SGC, 3 samples from the southern SGC, 3 samples from the West Qinling, and 4 samples from the Yidun terrane (Figures 3 and 4, S2–S4, and Tables S2 and S3 in the Data Set S1). The

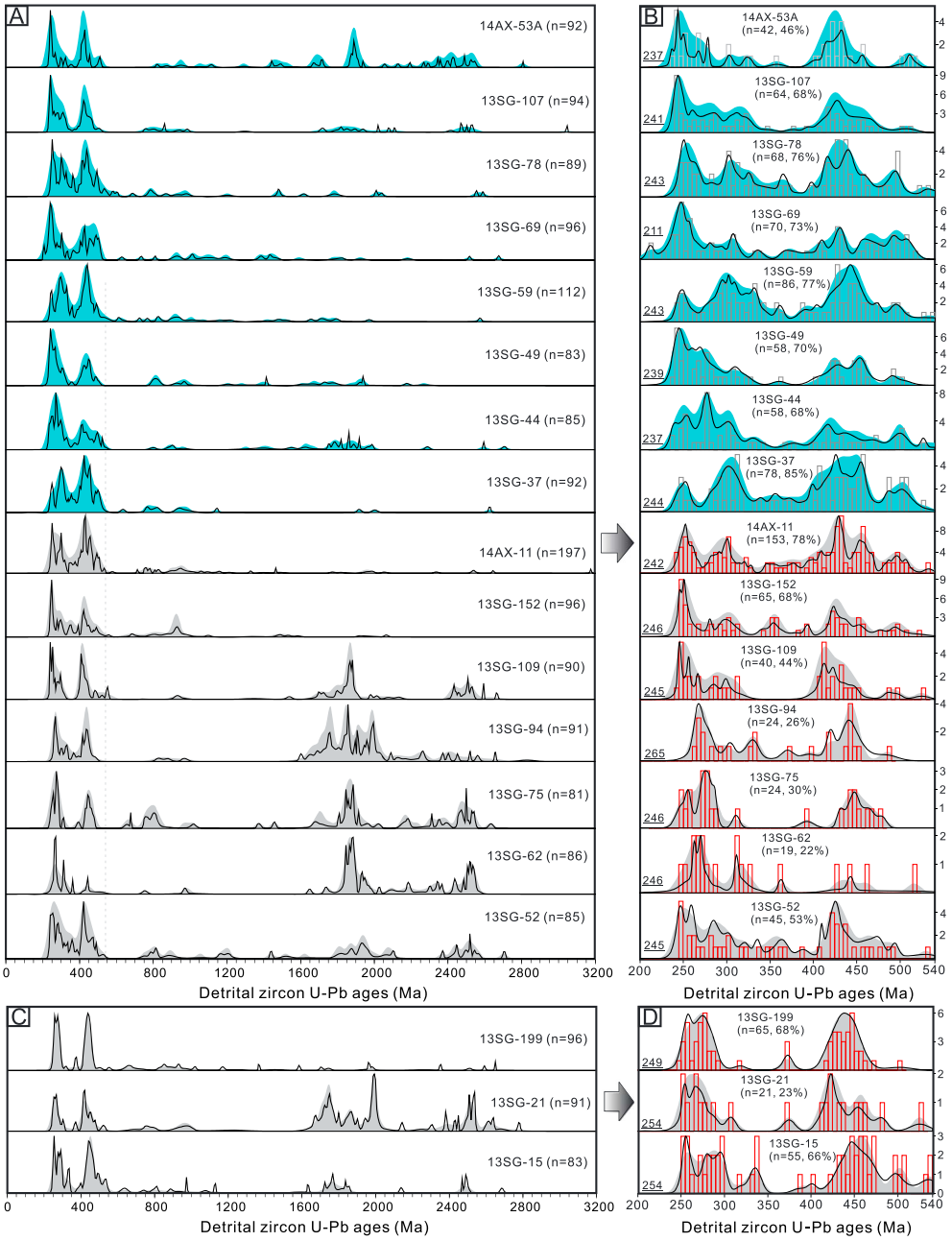

Figure 3. Detrital zircon U-Pb ages of the Triassic turbidite samples from the (a and b) central Songpan-Ganzi Complex and (c and d) West Qinling. The results indicate that these zircon ages are dominated by five populations: 240–310 Ma; 400–480 Ma; 750–1,000 Ma; 1,700–2,000 Ma; and 2,300–2,600 Ma. Note that most Middle Triassic samples are rich in Precambrian zircons with age peaks at 1,700–2,000 Ma and approximately 2,500 Ma, whereas the Late Triassic samples are dominated by Paleozoic zircons. The black lines represent probability density plots; the gray zones represent kernel density estimation plots of Middle Triassic samples; the green zones represent kernel density estimation plots of Late Triassic samples. All age plots (a) are drawn by using bandwidth = 20 in the DensityPlotter program (Vermeesch, 2012), while the Phanerozoic age plots (b) are drawn by using bandwidth = 8.

results indicate that most of the analyzed zircons have highly concordant $^{206}Pb/^{238}U$ and $^{207}Pb/^{235}U$ ages (Figures S3 and S4) and >98% zircons have U/Th ratios <10 (Figure S5). Furthermore, the relationship between zircon ages and U/Th ratios shows that the zircon grains with U/Th ratios >10 are mainly Early Paleozoic (420–500 Ma) and late Paleoproterozoic (1,800–2,000 Ma) in age (Figure S5). Overall, the turbidite detrital zircon ages in this study primarily consist of five populations: 240–310 Ma; 400–480 Ma;

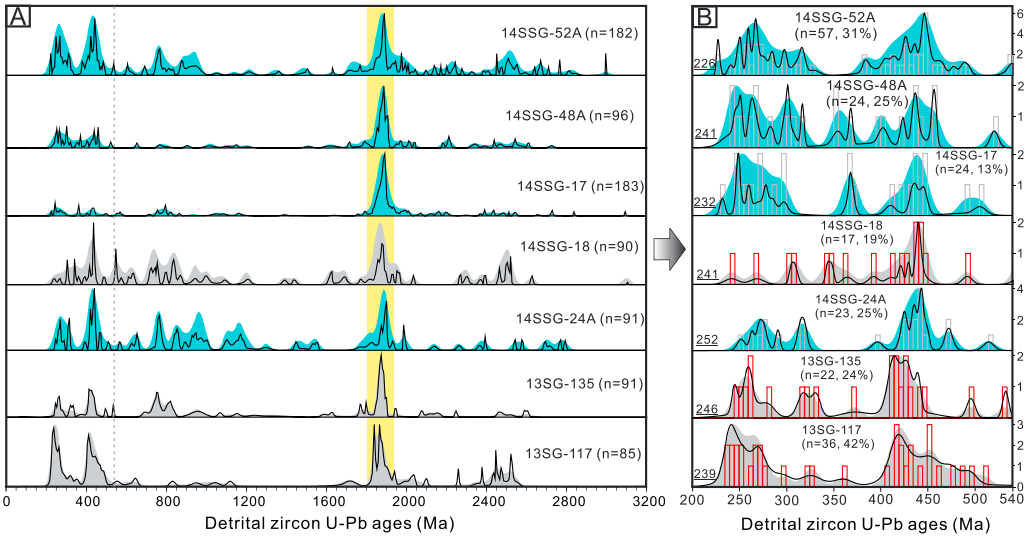

Figure 4. Comparison of detrital zircon U-Pb ages of southern Songpan-Ganzi Complex and Yidun turbidite samples. Note that the detrital zircon age spectra of all the samples are quite similar and are characterized by a significant age peak at approximately 1.85 Ga and most samples also have Neoproterozoic (750–1,000 Ma) zircon age peaks. The black lines represent probability density plots; gray zones represent kernel density estimation plots of Middle Triassic samples; the green zones represent kernel density estimation plots of Late Triassic samples.

750–1,000 Ma; 1,700–2,000 Ma; and 2,300–2,600 Ma ((Figures 3 and 4). The youngest detrital zircon ages from these samples, which represent the maximum depositional ages, vary from 275 Ma (Sample 13SG-94) to 211 Ma (Sample 13SG-69; Figures 3 and 4) and are consistent with the previously reported Middle-Late Triassic age of the flysch strata (Table 1).

The Middle Triassic West Qinling samples have similar detrital zircon ages with the Middle Triassic samples from the central SGC. These samples, excluding Samples 14AX-11, 13SG-152, and 13SG-199 (these three samples relatively close to the East Kunlun orogen), contain fairly large proportions of Precambrian zircons, and in particular, there are two major populations, that is, 1,700–2,000 Ma and 2,300–2,600 Ma (Figure 3). In contrast, the detrital zircons of the Upper Triassic samples from the central SGC with the exception of sample 14AX-53A, are dominated by Paleozoic to earliest Triassic ages, with major peaks at 240–310 Ma and 400–480 Ma, and subordinate peaks at 310–400 Ma (Table S4 in the Data Set S1). Almost every sample yielded Neoproterozoic age zircons, though the abundance of Neoproterozoic grains ranges from 3 to 25%. It is worth noting that the three Samples 13SG-117, 13SG-135, and 14SSG-24A from the southern margin of SGC are characterized by the age peak at approximately 1.85 Ga (but lack a major age peak at ~2.5 Ga that is more ubiquitous in other SGC sample). Furthermore, these southern SGC samples yield significant Neoproterozoic age peaks at approximately 750–850 Ma (Figures 4 and 5 and Table S4), which distinguishes them from the samples of northern and central regions that bear Neoproterozoic age peaks at approximately 900–950 Ma (Figure 3). The Yidun Group samples are dominated by Paleoproterozoic (age peak at approximately 1.85 Ga) and Neoproterozoic (age peaks at approximately 750–850) zircon populations and show relatively low abundances of Paleozoic zircons (except Sample 14SSG-52A). The zircon age distributions are very similar with the ones of southern SGC samples (Figure 4).

4.4. Potential Source Basement Metasedimentary Rock Detrital Zircon U-Pb Geochronology

We also report 594 detrital zircon U-Pb ages from four samples of basement composed of metasedimentary rock (Tables S2 and S3). Two samples from the East Kunlun and one sample from the Zhongza massif indicate dominant Neoproterozoic zircon ages, with the significant peak at approximately 930 Ma and 850 Ma (Figure 5), respectively. The sample from the Longmenshan thrust belt also has major zircon populations in Neoproterozoic ages, including 540–700 Ma, 750–800 Ma, and 950–1,000 Ma, and a population in early Paleoproterozoic-Neoarchean ages (Figure 5).

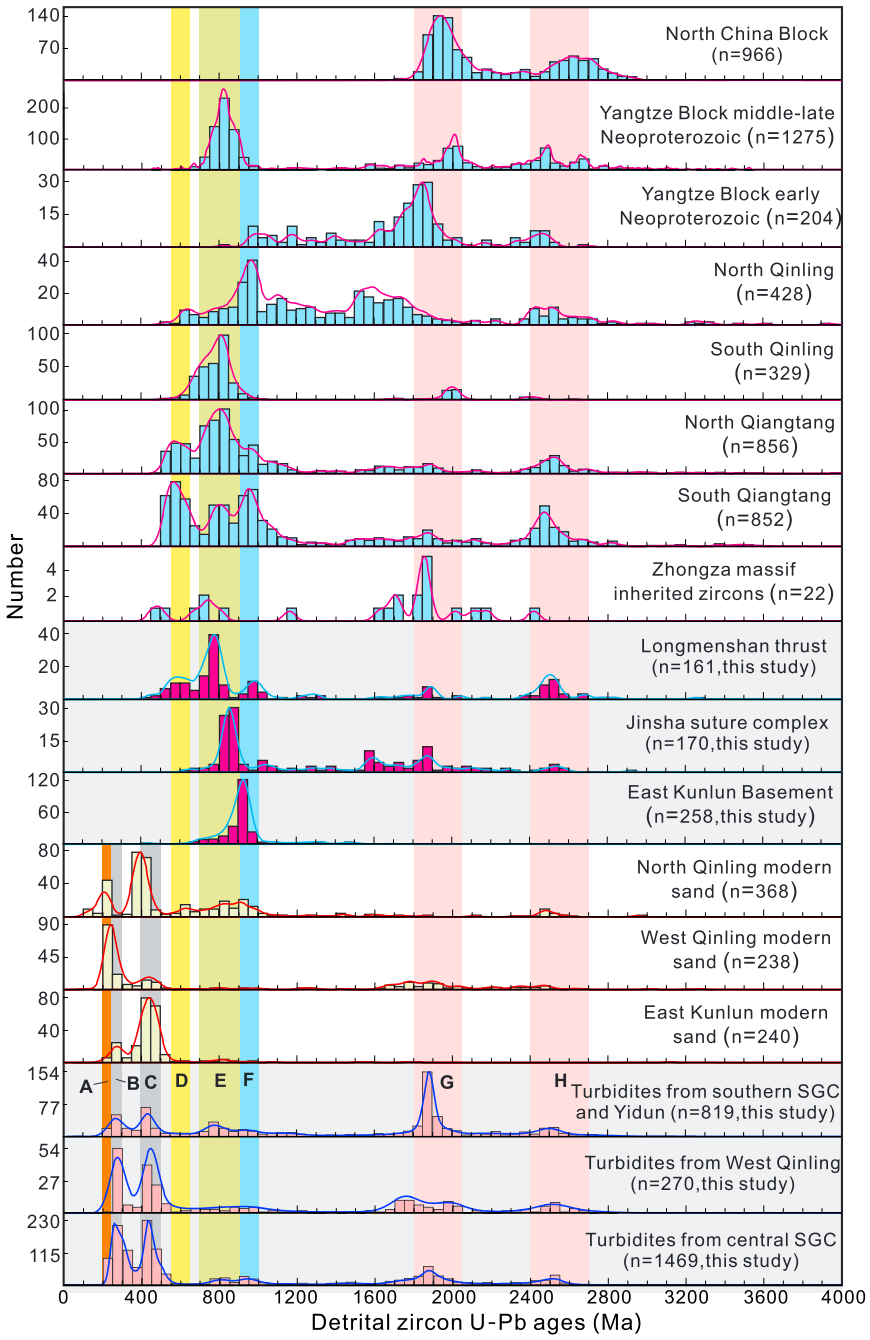

Figure 5. Detrital zircon age distributions of basement metasedimentary rocks analyzed in this study (red histogram) from the East Kunlun (Samples 13SG-158 and 14AX-26), Zhongza massif (14SSG-35), and Longmenshan thrust (14SSG-64) and the total Triassic turbidite samples from southern Songpan-Ganzi Complex (SGC) and Yidun terrane, West Qinling, and central SGC, compared with previous zircon dating results (in this study, data of Paleozoic and/or Precambrian sandstones and meta-sandstones and modern river sands were collected) from the surrounding potential source terranes. The zircon age populations marked as A-B, C, D, E-F, G, and H are employed to interpret the source areas. Therein, bimodal G and H ages zircons (with the peaks at approximately 1.85 Ga and 2.5 Ga) were likely from the NCB, unimodal G ages zircons were likely from the Zhongza massif, while the Neoproterozoic zircons (E-F) could be fed by the East Kunlun (might include Qaidam-Qilian), Qinling, Qiangtang terranes, Zhongza massif, and SCB. Zircons with D ages (540–700 Ma) were probably from Qiangtang block. The Phanerozoic zircons (A, B, and C) in the turbidites of north and central areas were most likely derived from East Kunlun (we suggest that the Qinling-Dabie belt served as the main source for the Triassic (A) detrital zircons), whereas the Phanerozoic zircons in the turbidites of southern SGC and Yidun were probably from Zhongza massif. Data of NCB (central and west areas) are from Darby and Gehrels (2006), Xia et al. (2006), and Tung, Yang, Yang, et al. (2007). Data of SCB (Yangtze) are from Liu et al. (2008) and Wang et al. (2010). Data of Central Qilian are from Gehrels et al. (2003, 2011) and Tung, Yang, Liu, et al. (2007). Data of North Qiangtang are from Pullen et al. (2008); Gehrels et al. (2011) and He et al. (2011). Data of South Qiangtang are from Gehrels et al. (2011). Data of South Qinling are from Ling et al. (2010). Data of North Qinling are from Diwu et al. (2010), Wan et al. (2011), and Zhu et al. (2011). Data of Zhongza massif are from Reid et al. (2007). For the modern sand data, signatures of East Kunlun, North Qinling, and West Qinling are collected from Li et al. (2013), Diwu et al. (2012), and Lease et al. (2007), respectively.

5. Interpretation and Discussion

Previous studies have reported a mass of petrographic and heavy mineral data for turbidite sandstones from West Qinling (Yan et al., 2014; Zhou & Graham, 1996), western SGC (Zhang et al., 2008), and the areas close to East Kunlun orogen (She et al., 2006). Those results demonstrate that the Triassic turbidites mainly had collision orogen and continental block sources. Our new petrographic data for the central SGC turbidite samples suggest a dominant orogenic source (Figure S1). Note that the framework petrography-based modal analysis and provenance interpretation would reflect a mixed signature if there were two or more types of sources. Although a lot of detrital zircon U-Pb geochronological data for the SGC turbidites had been published (Brugier et al., 1997; Ding et al., 2013; Weislogel et al., 2006, 2010; Y. X. Zhang et al., 2014), these studies provided distinct provenance interpretations (mentioned in the Introduction section). In this study, we combine newly acquired field-based paleocurrent data and detrital zircon U-Pb ages of central SGC samples to have a better understanding of the provenance and deep-water filling history of the eastern PTO.

5.1. Detrital Zircon Age Signatures of Potential Source Areas

Potential source areas for the SGC, Yidun, and West Qinling turbidites include the surrounding orogenic belts and blocks: East Kunlun, Qinling-Dabie, Qiangtang, Qilian, NCB, SCB, and Zhongza massif (Figure 1). Both published data of these regions and new detrital zircon U-Pb age data of basement metasedimentary rocks from the East Kunlun, Zhongza massif, and Longmenshan thrust belt are used to characterize potential source areas (Figure 5).

5.1.1. Potential Precambrian Zircon Source Areas

The NCB is characterized by Archean and Paleoproterozoic basement rocks, with reported zircon ages ranging from 1.6 to 3.0 Ga (e.g., Wilde et al., 2002); therein, zircons with approximately 1.8–2.0 Ga and approximately 2.5–2.6 Ga ages are the most common (e.g., Darby & Gehrels, 2006). The Mesoproterozoic-Neoproterozoic was a tectonic quiescence period in the NCB, and thus, few zircons were formed during this period (Figure 5).

In contrast, the SCB, Qinling, Qilian, and East Kunlun terranes are dominated by Neoproterozoic basement rocks, with the greatest zircon age probability peaks in the range of 750–1,000 Ma (Figure 5; Diwu et al., 2010, 2012; Gehrels et al., 2003; Liu et al., 2008; Wang et al., 2010; Yan et al., 2015). However, the age peaks in 750–1,000 Ma are slightly different for SCB (820 M), South Qinling (820 Ma), North Qinling (980 Ma), Qilian (800 Ma), and Kunlun terranes (940 Ma).

The Qiangtang terrane, which is considered to have Gondwana-affinity (Gehrels et al., 2011; He et al., 2011; Y. X. Zhang et al., 2014), also contains Neoproterozoic basement but with significant *Pan-African* (500–650 Ma) and Grenville (980–1200 Ma) zircons (Gehrels et al., 2011; He et al., 2011; Pullen et al., 2008). To that end, the presence of Qiangtang sourced detritus with Neoproterozoic age detrital zircons and an absence of Pan-African and Grenville age zircons would be unexpected.

The basement of Yidun terrane, thought to be represented by Zhongza massif (Figure 1), remains enigmatic. The Zhongza massif has been interpreted to be a microcontinent that rifted from the western Yangtze block during the Late Permian as evidenced by the Emeishan flood basalts (Hou, 1993; Song et al., 2004), whereas the Mediterranean-style rollback model suggests that the Yidun terrane was likely separated from the East Kunlun/Qinling belts prior to the Early-Middle Triassic (Pullen et al., 2008; L. Y. Zhang et al., 2014) The new zircon ages presented in this study, combined with results of Reid et al. (2007), indicate that the Yidun terrane basement mainly contains Neoproterozoic and Paleoproterozoic zircon, with the age peaks at approximately 850 Ma and 1.85 Ga (Figure 5).

5.1.2. Potential Phanerozoic Zircon Source Areas

The Phanerozoic age zircons are widely thought to have been sourced from the surrounding suture zones or orogenic belts, such as East Kunlun, Qinling-Dabie, and Jinsha and Ganzi-Litang sutures. Previous studies suggest that the East Kunlun experienced two major episodes of magmatic arc development with one during the early-middle Paleozoic (mainly including Ordovician and Silurian) and the other during the Permian-Early Triassic (e.g., Dai et al., 2013; Li et al., 2013). The episodes are interpreted as subduction and closure of Proto-Tethys and PTOs (Li et al., 2013), respectively. And two corresponding age populations, that is, 420–500 Ma and 250–290 Ma, primarily constitute the detrital zircon age spectra of the modern river sands at the foot of the East Kunlun orogenic belt (Li et al., 2013, Figure 5).

The Qinling-Dabie orogenic belt has the similar tectonic history as the East Kunlun. This orogen records Paleozoic and early Mesozoic convergence of NCB, SCB, North Qinling, and South Qinling microcontinents (Dong et al., 2011; Meng & Zhang, 2000). Major ages of magmatic events include early-middle Paleozoic (490–390 Ma), Middle Devonian-carboniferous (345–300 Ma), and Late Permian-Early Triassic (approximately 250–230 Ma; Dong et al., 2011; Meng & Zhang, 2000; Weislogel, 2008). The Phanerozoic zircons in modern river sands from Qinling-Dabie belt yield two main age populations at approximately 450–350 Ma and 250–230 Ma (Figure 5; Lease et al., 2007; Diwu et al., 2012).

The Jinsha and Ganzi-Litang sutures provide some record of the convergence and collision among SGC, Yidun, and Qiangtang terranes (Hou, 1993; Kapp et al., 2000, 2003; Zhang et al., 2006). The exposed granitic rocks in this region have zircon U-Pb ages at approximately 280–210 Ma (e.g., Reid et al., 2007; Weislogel, 2008; Yang et al., 2012, 2014; Peng et al., 2014). The closure of Jinsha suture between Qiangtang block and Yidun terrane is commonly regarded to have taken place by the Permian or Early-Middle Triassic (Reid et al., 2005, 2007; Yang et al., 2012, 2014), whereas the evolution of Ganzi-Litang suture is fairly complicated and remains enigmatic (see subsequent discussion).

5.2. Spatial and Temporal Provenance Variations of the Triassic Flysch and Implications for the Filling History

The combination of detrital zircon ages with paleocurrent data allows constraint of general regional paleotransport directions and predominant source areas. Because of the propensity of zircon to withstand multiple episodes of recycling, the absolute source of zircon grains cannot be determined. Thus, turbidite detrital zircon ages are interpreted in the context of paleocurrent orientations and probably include igneous rocks and associated cover strata. Note that most separated zircon grains are angular to subangular (Figure S2), implying the predominance of first-cycle deposition and short transport distance. This inference is consistent with the petrography results, which indicate that the analyzed turbidite sandstones are dominated by angular to subangular and poorly to moderately sorted framework grains (Figure S1).

According to the zircon age signatures of the potential source areas mentioned above, detrital zircon provenance for the analyzed Triassic samples can be interpreted as follows. For the West Qinling and central SGC samples, the Paleoproterozoic and Neoarchean zircons with bimodal age peaks at approximately 1.85 and 2.5 Ga (Figure 3 and Table S4) were likely derived from the NCB basement (Figure 5), whereas the Neoproterozoic zircons with an age peak at approximately 930 Ma (Figure 3 and Table S4) were probably derived from the East Kunlun basement rather than SCB or Qiangtang terrane (Figure 5). The Paleozoic and Early Triassic zircons in these samples were from East Kunlun with subordinate contribution from the Qinling-Dabie, therein the Qinling-Dabie orogenic belt likely served as the major source for the Late Devonian-Carboniferous (300–380 Ma) zircons (Ratschbacher et al., 2003). This interpretation is also reinforced by the dominantly south and southwest directed paleoflow (Figure 2). Detrital zircons of several Middle Triassic samples near the East Kunlun (e.g., Samples 13SG-152, 13SG-199, and 14AX-11) are dominated by Paleozoic and Neoproterozoic ages, implies that the East Kunlun probably served as the major source for these turbidites. The Middle Triassic samples from the central SGB and West Qinling (i.e., Samples 13SG-62, 13SG-75, 13SG-52, 13SG-109, 13SG-15, and 13SG-21) are characterized by high abundances of Paleoproterozoic and Neoarchean zircons (up to 70%), revealing high contributions of the NCB, whereas Upper Triassic samples (i.e., Samples 13SG-37, 13SG-59, 13SG-49, 13SG-78, 13SG-44, 13SG-69, and 13SG-107) primarily consist of Paleozoic zircons (Figures 3 and 6). These results suggest that detritus supply from NCB was highly reduced or diluted by major contribution from East Kunlun since the Late Triassic. These conclusions are consistent with the framework petrography modal analysis results, which indicate a dominant collision orogen and suture source for these turbidites (Figure S1).

The Middle-Late Triassic samples from the southern SGC (i.e., Samples 13SG-117, 13SG-135, and 14SSG-24A) and Yidun terrane (i.e., Samples 14SSG-17, 14SSG-18, 14SSG-48A, and 14SSG-52A) have fairly similar detrital zircon age distributions (Figure 4), which indicate the most significant Paleoproterozoic age population in the range of 1.8–1.95 Ga (with the unimodal peak at approximately 1.85 Ga). The detrital zircon age similarity (Figure 4) and overwhelmingly north and northeast directed paleocurrents (Figure 2) reveal that these turbidites likely shared the same and invariable sources during the Middle-Late Triassic. Since the Yidun terrane (including Zhongza massif) contains Neoproterozoic (this study, with the age peak at approximately 820 Ma) and Paleoproterozoic (with the age peak at approximately 1.85 Ga) basement

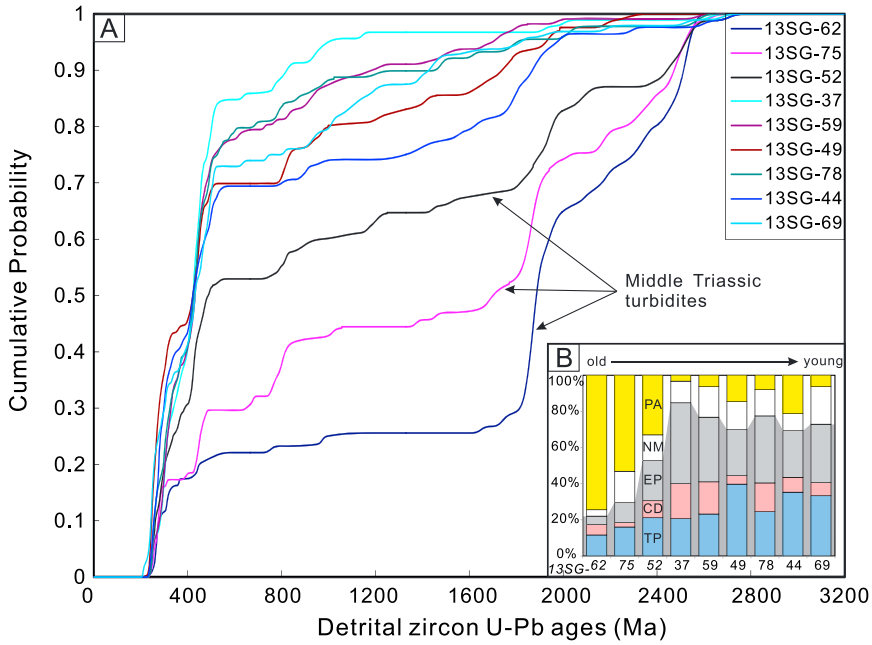

Figure 6. (a) Detrital zircon U-Pb age cumulative probability distributions and (b) stratigraphic variations of Triassic turbidite samples from the Dari Section (in the central Songpan-Ganzi Complex; Figure 1). Note that the Late Triassic samples distinctly have less Paleoproterozoic and Archean zircons and more Phanerozoic zircons than the Middle Triassic samples. PA: Paleoproterozoic and Archean age (>1,600 Ma); NM: Neoproterozoic and Mesoproterozoic age (540–1,600 Ma); EP: Early Paleozoic age (400–540 Ma); CD: Carboniferous and Devonian age (310–400 Ma); TP: Triassic and Permian age (200–310 Ma).

rocks (Reid et al., 2007), it may have been the source for many of the Precambrian zircons of similar age observed in the southern SGC and Yidun turbidite samples (Figure 5). The Yangtze block was also a potential source for the Neoproterozoic detrital zircons, as some turbidite locations in southern SGC reveal west directed paleoflow (Figure 2; Weislogel et al., 2006, 2010). Pan-African age zircons are not obviously observed in the analyzed samples; thus, the Qiangtang terrane is an unlikely contributor to these turbidites. Although only Permian-Triassic arc rocks are exposed in the current Yidun terrane and Jinsha suture zone (Peng et al., 2014; Reid et al., 2007; Weislogel, 2008; Yang et al., 2012, 2014), our newly obtained detrital zircon age data (unpublished) of Permian strata in the Yidun terrane indicate dominant early Paleozoic and Neoproterozoic age populations. Hence, Paleozoic zircons of the southern SGC and Yidun turbidites were also likely derived from Pre-Triassic basement of Yidun terrane and the Jinsha suture zone. This conclusion is reinforced by previous structural analyses in that area, which suggest Early Triassic deformation of Paleozoic sequences in the Yidun terrane resulting from the Jinsha suture closure (Reid et al., 2005). However, Ding et al. (2013) and Wang, Wang, et al. (2013) obtained very different detrital zircon geochronological results for Yidun Group turbidites, which show major early Paleozoic and Neoproterozoic age populations and the minimum detrital zircon age of Early Devonian. Since the closure of the Jinsha suture between Yidun and Qiangtang terranes have occurred by the Permian or Early-Middle Triassic (Reid et al., 2005, 2007; Yang et al., 2012, 2014) and there was emplacement of widespread Early-Middle Triassic granitoids in the western Yidun terrane (Reid et al., 2007), we suggest that the data of those samples (Ding et al., 2013; Wang, Wang, et al., 2013) should be interpreted with caution. Alternatively, those samples might be from pre-Triassic sequence in the Yidun terrane. This uncertainty encourages a more detailed investigation of Yidun Triassic turbidites.

5.3. Triassic Tectonic Evolution and Closure of the Eastern PTO

5.3.1. Pre-Middle Triassic Aggregation of SGC and Yidun Terrane

This study shows that turbidites of the southern SGC and Yidun terrane have similar detrital zircon age spectra (Figure 7) and show similar paleocurrent orientations (Figure 2). We cannot exclude the occurrence of recycling from the Yidun turbidite strata to the southern SGC turbidites, but considering the Yidun Group

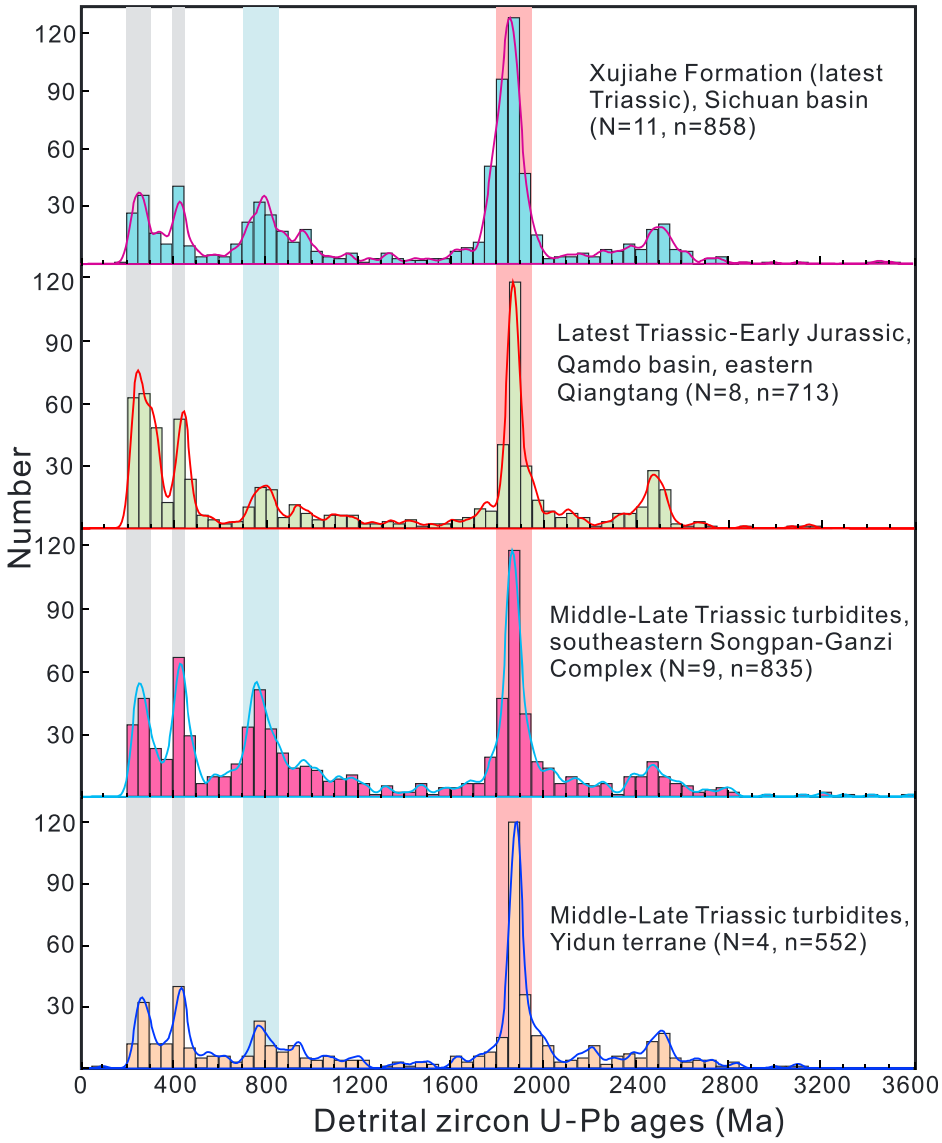

Figure 7. Detrital zircon U-Pb age distribution comparison (kernel density estimation plots) of Middle-Late Triassic turbidites in the southeastern Songpan-Ganzi Complex (Ding et al., 2013; Weislogel et al., 2010; and this study), Middle-Late Triassic turbidites in the Yidun terrane (all data are from this study), latest Triassic-Early Jurassic sandstones of Qamdo basin, eastern Qiangtang (Shang, 2016), and the Xujiahe Formation sandstones of western Sichuan basin (Luo et al., 2014; Weislogel et al., 2010).

strata and the southern SGC turbidite strata was likely deposited during the same time, we favor the scenario that these two depocenters were adjacent to each other and had similar source areas and transport pathways. This means that aggregation of SGC and Yidun terrane and the closure of Ganzi-Litang Ocean probably had to have occurred by the Middle Triassic.

The sedimentological argument is not consistent with the conclusion of most previous studies, which advocated that the Late Triassic igneous rocks in eastern Yidun terrane were the products of subduction-related arc magmatism (e.g., Roger et al., 2010; Yang et al., 2012, 2014). Therein, Roger et al. (2010) proposed that these Late Triassic igneous rocks resulted from east dipping subduction of the Jinsha Ocean, whereas Hou (1993) and Wang et al. (2011) suggested west dipping subduction of the Ganzi-Litang Ocean. Our results do not support an oceanic trench and a subduction zone in the east margin of Yidun terrane, even a trench in the west margin during the Late Triassic, because rocks exposed what is now the Jinsha suture zone are

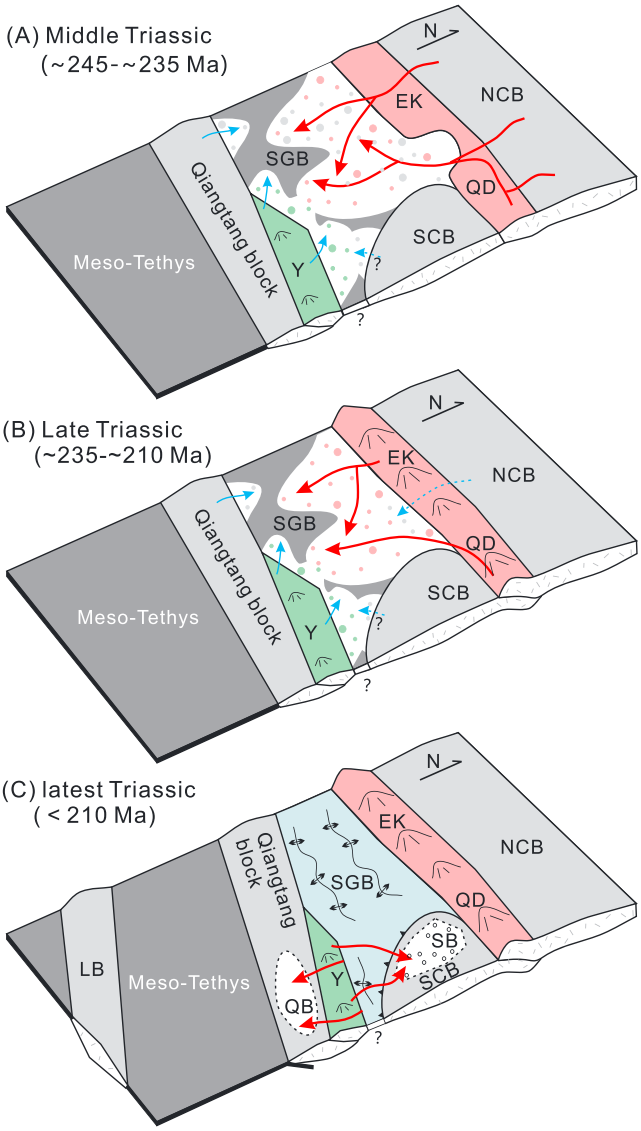

Figure 8. Sketched model illustrating the basin filling history and tectonic evolution of the SGC and surrounding areas. (a) During the Middle Triassic, the SGB was dominantly fed by materials from the NCB, East Kunlun, while SCB, Qiangtang block and Yidun terrane (Zhongza massif) served as minor source areas for locally south and southeast depocenters (the red arrows indicate the primary sediment transport pathways). We contend that East Kunlun (and Qinling-Dabie) area showed relatively low relief topography during this period. (b) During the Late Triassic, the East Kunlun is favored as the main source area, whereas the NCB became a minor source, indicating the tectonic uplift, high-relief landscape, and more exposure of the East Kunlun rocks. (c) Since the latest Triassic (likely <210 Ma), the turbidite strata of the SGC and Yidun terrane were deformed and exhumed and fed the Sichuan basin to the east and Qamdo basin to the west. NCB: North China block; SCB: South China block; SGB: Songpan-Ganzi basin; EK: East Kunlun; QD: Qinling-Dabie; QB: Qiangtang block; Y: Yidun; SB: Sichuan basin; LB: Lhasa block.

the most likely sources for the southern SGC and Yidun turbidites. Furthermore, Peng et al. (2014) suggested that an arc setting could be argued against due to the coeval occurrence of the Late Triassic intrusive rocks on both sides of the Ganzi-Litang suture; alternatively, they proposed a postorogenic collapse model for the Mesozoic magmatism in the Yidun terrane. This means that the collision between Yidun and SGC and subsequent orogenesis had been completed by the Middle Triassic and the turbidite deposition there predated the formation of these igneous rocks.

5.3.2. Late Triassic Uplift and Exhumation of East Kunlun

Similarly, the Triassic West Qinling and central SGC depocenters were likely adjacent to each other and shared the same detritus sources, due to the similarity of detrital zircon ages of Middle Triassic samples from these two areas (Figure 3). This implies that the A'nyemaqen ocean basin, as a branch of the PTO (Bian et al., 2004; Guo et al., 2007), should be closed prior to the Middle Triassic. The temporal variations of detrital zircon age spectra for the central SGC samples suggest a decreasing proportional contribution of NCB from Middle Triassic to Late Triassic (Figure 6), implying relatively more exposure and erosion of the East Kunlun and/or cutting off of detritus transport from the NCB since the Late Triassic. This suggests that the East Kunlun, located on northern margin of the eastern PTO, probably underwent a significant Late Triassic uplift and exhumation event, which resulted in more exposure of the Paleozoic rocks in this area. This conclusion is consistent with the previous thermochronological studies of the East Kunlun (e.g., Dai et al., 2013; Jolivet et al., 2001; Liu et al., 2005; Mock et al., 1999). The first set of Late Triassic cooling ages (224–219 Ma) were obtained by Mock et al. (1999), based on the $^{40}Ar/^{39}Ar$ data of K-feldspar of Paleozoic granitoids. A great number of Late Triassic $^{40}Ar/^{39}Ar$ age (approximately 240–215 Ma) of biotite and muscovite were also detected by Liu et al. (2005), on the basis of basement metamorphic rocks. Jolivet et al. (2001) suggested a general Late Triassic-Early Jurassic cooling event constrained by zircon fission-track ages ranging from 221 to 96 Ma, which include several Late Triassic ages with the range of 221–203 Ma. Furthermore, a Late Triassic zircon (U-Th)/He age (215 Ma) of Paleozoic granitoids was also acquired recently (Dai et al., 2013). Combining the corresponding apatite (U-Th)/He age, a rapid cooling rate of ~19 °C/Ma during the Late Triassic and Early Jurassic was calculated, which indicates an early Mesozoic stage of rapid exhumation (~0.8 km/Ma; Dai et al., 2013). All the evidence demonstrates that the East Kunlun area experienced a rapid uplift and exhumation event since the Late Triassic. And the high rate of exhumation and erosion and potentially high relief topography there did not only lead to the major source of East Kunlun for the turbidites but also resulted in abundant detritus supply for a fairly large depositional area (Figure 8).

5.3.3. Latest Triassic Deformation and Denudation of the Triassic Songpan-Ganzi and Yidun Flysch

The deformation of the SGC and Yidun flysch, which is characterized by tightly folded strata with vertical/subvertical NW-SE striking axial planes (e.g., Burchfiel et al., 1995; Reid et al., 2005; Roger et al., 2004, 2010; Xu et al., 1992), has attracted much attention for decades. This deformational event is generally regarded to be contemporaneous with collision and subsequent continuing convergence between NCB and SCB (Burchfiel et al., 1995; Yin & Harrison, 2000; Yin & Nie, 1996). The timing of the deformation is constrained by the emplacement of synkinematic and postkinematic granites, which yield the ages of approximately 215–190 Ma (e.g., de Sigoyer et al., 2014; Roger et al., 2004; Weislogel,

2008; L. Y. Zhang et al., 2014). Furthermore, a late Indosinian (~205–190 Ma) tectonometamorphic event and related crustal thickening and shortening were previously recognized in the Danba domal metamorphic terrane in the eastern SGC (Huang et al., 2003). According to the comparison of detrital zircon age spectra (Figure 7), the Middle-Upper Triassic turbidites in southern SGC and Yidun terrane are proposed to be major sources for latest Triassic sediments (i.e., Xujiahe Formation) of the Sichuan basin to the east and for the latest Triassic and Early Jurassic sediments (i.e., Bagang and Chaya Groups) of the Qamdo basin (eastern Qiangtang) to the west (Figure 8). The details of the Qamdo basin provenance interpretations were provided by Shang (2016). For the Sichuan basin, there is more direct or indirect evidence supporting this conclusion. First, the youngest detrital zircon ages (approximately 212–207 Ma) of sandstone samples of the Xujiahe Formation (e.g., Liu et al., 2015; Luo et al., 2014) indicate that the Xujiahe Formation deposition was later than the SGC flysch deposition and subsequent deformation. Second, the flexural foreland basin feature of the latest Triassic Sichuan basin (Meng et al., 2005; Yong et al., 2003) supports that the source region should be located in the west of the basin (i.e., Longmenshan area and southeastern SGC or larger regions). Third, the source to the west is also reinforced by sedimentary environment transformation (from Early-Middle Triassic shallow-marine environment to Late Triassic terrestrial deposition) and paleocurrents (Meng et al., 2005).

Importantly, it is worth noting that the detrital zircon age spectra of the Xujiahe Formation sandstones (Liu et al., 2015; Luo et al., 2014; Weislogel et al., 2010) are very different from the zircon age spectra of the Paleozoic strata (e.g., Sample 14SSG-64 in this study) of the Longmenshan thrust area (Figures 5 and 7; Chen et al., 2018; Duan et al., 2011; and our unpublished data). This means that the Paleozoic rocks currently exposed in the Longmenshan area were not likely sources for the latest Triassic deposits in the Sichuan basin (also not sources for the Triassic southern SGC turbidites). Sediment deposited in the Sichuan flexural foreland during the latest Triassic was sourced from southern SGC affinity Triassic sediments rather than northeastern and central SGC, at present exposed in the hinterland of the Longmenshan thrust belt (Burchfiel et al., 1995). Hence, we suggest that the Paleozoic sequence in the Danba area served as the pre-Triassic basement for the SGC terrane and was probably covered by Triassic turbidites of southern SGC affinity prior to the latest Triassic deformation. This suggestion is consistent with the structural analyses of southern SGC and Danba antiform area (Harrowfield & Wilson, 2005), which recommend two stages of folding history for the flysch and underlying basements, divided by a ductile décollement at the base of the sedimentary pile. If we assume that the erosion and recycling of the turbidites were triggered by the SGC folding and invert, the results of this study also imply that the SGC deformation was likely coeval with or predated the shortening within the Longmenshan thrust belt. Therefore, the data presented here are probably at odds with the Mediterranean-style model proposed by Pullen et al. (2008), which predicts that the shortening in the Longmenshan area during the Late Triassic would have been primarily driven by rollback of Paleo-Tethys oceanic lithosphere beneath the *allochthonous* block of the Longmenshan and thus predated the SGC deformation. Besides, the Paleozoic strata of the Longmenshan thrust belt and the pre-Triassic basement of the SGC have different detrital zircon ages and thus distinct tectonic evolutionary histories with the Paleozoic East Kunlun-Qinling orogenic belt (Figures 5; Duan et al., 2011; Chen et al., 2018; and our unpublished data). This is also inconsistent with the rollback model, which assumes that the allochthonous Longmenshan and the pre-Triassic SGC fragments were separated from the East Kunlun-Qinling orogenic belt (L. Y. Zhang et al., 2014).

5.4. Implications for Synorogenic Sedimentation in Deep Oceans

While the relation of the modern Bengal fan to the Cenozoic Himalayan suture belt (resulted from the India-Eurasia collision) suggests a guiding principle of synorogenic sedimentation (Copeland & Harrison, 1990; Ingersoll et al., 2003; Uddin & Lundberg, 1998), the thick and widespread Triassic flysch in the SGC, eastern Tibet, provides a typical example of ancient synorogenic sedimentation systems. An analogue is the Carboniferous-Permian Ouachita-Marathon flysch deposits of Arkansas, Oklahoma, and Texas in the North America (Graham et al., 1975; Ingersoll et al., 2003). Although the Triassic tectonic setting of the Songpan-Ganzi oceanic basin remains debatable (Ding et al., 2013; Pullen et al., 2008; Weislogel et al., 2006; L. Y. Zhang et al., 2014), it is well acceptable that the eastern PTO received a heavy load of detritus from the surrounding active collisional orogenic belts and the collided continents (e.g., She et al., 2006; Weislogel et al., 2006; Y. X. Zhang et al., 2014 and this study). As the SGC shown, the ancient synorogenic

deposits are currently preserved as highly deformed accretionary masses that contribute significantly to the building of the plateau and the continental crust. Their recognition as such is a significant step in our understanding of the creation and recycling of continental crust.

6. Conclusions

This study combines field-based paleocurrent, petrography, and detrital zircon geochronological data of Middle-Upper Triassic turbidites from the central SGC, Yidun, and West Qinling terranes and yields the following conclusions concerning Triassic flysch provenance and late tectonic evolution of the eastern PTO:

1. Petrographic investigation indicates that the turbidites have relatively low textural and compositional maturity, with some samples experiencing low-grade metamorphism. The modal analysis of framework grain composition suggests that these turbidite sandstones have an overwhelming derivation from an orogen source.
2. The detrital zircon ages obtained in these turbidites primarily consist of five populations: 240–310 Ma; 400–480 Ma; 750–1,000 Ma; 1,700–2,000 Ma; and 2,300–2,600 Ma. Based on the age comparison of turbidites and potential sources, incorporating paleocurrent data, we suggest that the central SGC and West Qinling turbidites were dominantly derived from the East Kunlun and NCB, whereas the turbidites of southern SGC and Yidun terrane were mainly fed by the basement of Yidun terrane and Jinsha suture.
3. The similarity of detrital zircon ages of the Middle-Upper Triassic southern SGC and Yidun turbidites and overwhelmingly north and northeast directed paleocurrents imply that the aggregation between SGC and Yidun terranes and the closure of Ganzi-Litang Ocean probably have occurred by the Middle Triassic.
4. The East Kunlun probably contributed more materials for Upper Triassic turbidites than Middle Triassic turbidites. This implies that the East Kunlun, located on northern margin of the eastern PTO, probably experienced a rapid uplift and exhumation event during the Late Triassic, which resulted in relatively high-relief landscape and more exposure of Paleozoic rocks.
5. We contend that the Triassic flysch in the southern SGC and Yidun terranes were major sources for the latest Triassic sediments of Sichuan basin to the east and Qamdo basin (eastern Qiangtang) to the west. And the Longmenshan area is suggested to be covered by Triassic turbidites at that time, which implies that the deformation of the SGC was likely coeval with or predated the latest Triassic shortening in the Longmenshan thrust belt.

Acknowledgments
This work was supported by the National Natural Science Foundation of China (41806052), the Natural Science Foundation of Fujian Province (2017J05067), and U.S. National Science Foundation grants (EAR-1118908 and EAR-1118525). We would like to thank Wei Zhang, Delores Robinson, Will Jackson Jr., and Lin Li for assistance during the field work. We appreciate Fei Shang for providing raw detrital zircon age data of the Qamdo basin samples. George Gehrels, Mark Pecha, Nicky Giesler, Sonnet Gomes, Russ Linger, Jon Campbell, and Sam Bowman are thanked for their help on the zircon U-Pb dating. Olivier Vanderhaeghe and another two anonymous reviewers are appreciated for their helpful and constructive suggestions. All data are provided in the present manuscript and supporting information Figures S1 (turbidite sandstone representative micrographs and Q-F-L plots), S2 (selected detrital zircon BSE images), S3 and S4 (detrital zircon U-Pb age concordia diagrams), and S5 (detrital zircon U/Th ratios) and Tables S1 (sandstone petrography), S2 (sample information), S3 (detrital zircon U-Pb geochronology), and S4 (detrital zircon age peak characteristics).

References

Bian, Q. T., Li, D. H., Pospelov, I., Yin, L. M., Li, H. S., Zhao, D. S., et al. (2004). Age, geochemistry and tectonic setting of Buqingshan ophiolites, north Qinghai-Tibet Plateau, China. *Journal of Asian Earth Sciences*, *23*(4), 577–596. https://doi.org/10.1016/j.jseaes.2003.09.003

Billerot, A., Duchene, S., Vanderhaeghe, O., & de Sigoyer, J. (2017). Gneiss domes of the Danba Metamorphic Complex, Songpan Ganze, eastern Tibet. *Journal of Asian Earth Sciences*, *140*, 48–74. https://doi.org/10.1016/j.jseaes.2017.03.006

Brugier, O., Lancelot, J. R., & Malavieille, J. (1997). U-Pb dating on single zircon grains from the Triassic Songpan–Garze flysch (Central China): Provenance and tectonic correlations. *Earth and Planetary Science Letters*, *152*(1–4), 217–231. https://doi.org/10.1016/S0012-821X(97)00138-6

Burchfiel, B. C., Chen, Z., Liu, Y., & Royden, L. H. (1995). Tectonics of the Longmen Shan and adjacent regions, central China. *International Geology Review*, *37*(8), 661–735. https://doi.org/10.1080/00206819509465424

Bureau of Geology and Mineral Resources of Qinghai Province (BGMRQP) (1991). *Regional geology of Qinghai Province* (in Chinese with English abstract). Beijing: Geological Publishing House.

Bureau of Geology and Mineral Resources of Sichuan Province (BGMRSP) (1991). *Regional geology of Sichuan Province* (in Chinese with English abstract). Beijing: Geological Publishing House.

Cai, H. M., Zhang, H. F., Xu, W. C., Shi, Z. L., & Yuan, H. L. (2010). Petrogenesis of Indosinian volcanic rocks in Songpan-Garze fold belt of the northeastern Tibetan Plateau: New evidence for lithospheric delamination. *Science in China Series D: Earth Sciences*, *52*(9), 1316–1328. https://doi.org/10.1007/s11430-010-4033-9

Chang, E. Z. (2000). Geology and tectonics of the Songpan-Ganzi fold belt, southwestern China. *International Geology Review*, *42*(9), 813–831. https://doi.org/10.1080/00206810009465113

Chen, Q., Sun, M., Long, X., Zhao, G., Wang, J., Yu, Y., & Yuan, C. (2018). Provenance study for the Paleozoic sedimentary rocks from the west Yangtze Block: Constraint on possible link of South China to the Gondwana supercontinent reconstruction. *Precambrian Research*, *309*, 271–289. https://doi.org/10.1016/j.precamres.2017.01.022

Chen, Z., Burchfiel, B. C., Liu, Y., King, R. W., Royden, L. H., Tang, W., et al. (2000). Global positioning system measurements from eastern Tibet and their implications for India/Eurasia intercontinental deformation. *Journal of Geophysical Research*, *105*, 16,215–16,227. https://doi.org/10.1029/2000JB900092

Cogné, J. P., Halim, N., Chen, Y., & Courtillot, V. (1999). Resolving the problem of shallow magnetizations of Tertiary age in Asia: Insights from paleomagnetic data from the Qiangtang, Kunlun, and Qaidam blocks (Tibet, China), and a new hypothesis. *Journal of Geophysical Research*, *104*, 17,715–17,734. https://doi.org/10.1029/1999JB900153

Copeland, P., & Harrison, T. M. (1990). Episodic rapid uplift in the Himalayas revealed by 40Ar/39Ar analysis of detrital K-feldspar and muscovite, Bengal fan. *Geology*, *18*(4), 354–357. https://doi.org/10.1130/0091-7613(1990)018<0354:ERUITH>2.3.CO;2

Dai, J., Wang, C., Hourigan, J., & Santosh, M. (2013). Multi-stage tectono-magmatic events of the Eastern Kunlun Range, northern Tibet: Insights from U–Pb geochronology and (U–Th)/He thermochronology. *Tectonophysics*, *599*, 97–106. https://doi.org/10.1016/j.tecto.2013.04.005

Darby, B. J., & Gehrels, G. (2006). Detrital zircon reference for the North China Block. *Journal of Asian Earth Science*, *26*(6), 637–648. https://doi.org/10.1016/j.jseaes.2004.12.005

de Sigoyer, J., Vanderhaeghe, O., Duchêne, S., & Billerot, A. (2014). Generation and emplacement of Triassic granitoids within the Songpan Ganze accretionary-orogenic wedge in a context of slab retreat accommodated by tear faulting, Eastern Tibetan plateau, China. *Journal of Asian Earth Sciences*, *88*, 192–216. https://doi.org/10.1016/j.jseaes.2014.01.010

Dickinson, W. R. (1985). Interpreting provenance relations from detrital modes of sandstones. In G. G. Zuffa (Ed.), *Provenance of Arenites* (pp. 333–336). Dordrecht: Reidel.

Ding, L., Yang, D., Cai, F. L., Pullen, A., Kapp, P., Gehrels, G. E., et al. (2013). Provenance analysis of the Mesozoic Hoh-Xil-Songpan-Ganzi turbidites in northern Tibet: Implications for the tectonic evolution of the eastern Paleo-Tethys Ocean. *Tectonics*, *32*, 34–48. https://doi.org/10.1002/tect.20013

Diwu, C. R., Sun, Y., Liu, L. A., Zhang, C. L., & Wang, H. L. (2010). The disintegration of Kuanping Group in North Qinling orogenic belts and Neo-proterozoic N-MORB. *Acta Petrologica Sinica*, *26*, 2025–2038.

Diwu, C. R., Sun, Y., Zhang, H., Wang, Q., Guo, A. L., & Fan, L. G. (2012). Episodic tectonic thermal events of the western North China Craton and North Qinling Orogenic Belt, in central China: Constraints from detrital zircon U–Pb ages. *Journal of Asian Earth Sciences*, *47*, 107–122. https://doi.org/10.1016/j.jseaes.2011.07.012

Dong, Y. P., Zhang, G. W., Neubauer, F., Liu, X. M., Genser, J., & Hauzenberger, C. (2011). Tectonic evolution of the Qinling orogen, China: Review and synthesis. *Journal of Asian Earth Sciences*, *41*(3), 213–237. https://doi.org/10.1016/j.jseaes.2011.03.002

Duan, L., Meng, Q. R., Zhang, C. L., & Liu, X. M. (2011). Tracing the position of the South China block in Gondwana: U–Pb ages and Hf isotopes of Devonian detrital zircons. *Gondwana Research*, *19*(1), 141–149. https://doi.org/10.1016/j.gr.2010.05.005

Dupont-Nivet, G., Butler, R. F., Yin, A., & Chen, X. (2002). Paleomagnetism indicates no Neogene rotation of the Qaidam basin in north Tibet during Indo-Asian collision. *Geology*, *30*(3), 263–266. https://doi.org/10.1130/0091-7613(2002)030<0263:PINNRO>2.0.CO;2

Faure, M., Lin, W., & Le Breton, N. (2001). Where is the North China-South China block boundary in eastern China? *Geology*, *29*(2), 119–122. https://doi.org/10.1130/0091-7613(2001)029<0119:WITNCS>2.0.CO;2

Gehrels, G., Kapp, P., DeCelles, P., Pullen, A., Blakey, R., Weislogel, A., et al. (2011). Detrital zircon geochronology of pre-tertiary strata in the Tibetan-Himalayan orogen. *Tectonics*, *30*, TC5016. https://doi.org/10.1029/2011TC002868

Gehrels, G., Yin, A., & Wang, X. (2003). Detrital-zircon geochronology of the northeastern Tibetan Plateau. *Geological Society of America Bulletin*, *115*(7), 881–896. https://doi.org/10.1130/0016-7606(2003)115<0881:DGOTNT>2.0.CO;2

Gehrels, G. E., Valencia, V., & Ruiz, J. (2008). Enhanced precision, accuracy, efficiency, and spatial resolution of U–Pb ages by laser ablation–multicollector–inductively coupled plasma–mass spectrometry. *Geochemistry, Geophysics, Geosystems*, *9*, Q03017. https://doi.org/10.1029/2007GC001805

Graham, S. A., Dickinson, W. R., & Ingersoll, R. V. (1975). Himalayan-Bengal model for flysch dispersal in the Appalachian-Ouachita system. *Geological Society of America Bulletin*, *86*(3), 273–286. https://doi.org/10.1130/0016-7606(1975)86<273:HMFFDI>2.0.CO;2

Guo, A., Zhang, G., Sun, Y., Zheng, J., Liu, Y., & Wang, J. (2007). Geochemistry and spatial distribution of OIB and MORB in A'nyemaqen ophiolite zone: Evidence of Majixueshan ancient ridge-centered hotspot. *Science in China Series D: Earth Sciences*, *50*(2), 197–208. https://doi.org/10.1007/s11430-007-0197-3

Hacker, B. R., Ratschbacher, L., & Liou, J. G. (2004). Subduction, collision and exhumation in the ultrahigh-pressure Qinling–Dabie orogen. *Geological Society, London, Special Publications*, *226*(1), 157–175. https://doi.org/10.1144/GSL.SP.2004.226.01.09

Halim, N., Cogné, J. P., Chen, Y., Atasiesi, R., Besse, J., Courtillot, V., Gilder, S., et al. (1998). New Cretaceous and early Tertiary paleomagnetic results from Xining-Lanzhou basin, Kunlun and Qiangtang blocks, China: Implications on the geodynamic evolution of Asia. *Journal of Geophysical Research*, *103*, 21,025–21,045. https://doi.org/10.1029/98JB01118

Harrowfield, M. J., & Wilson, C. J. (2005). Indosinian deformation of the Songpan Garze fold belt, northeast Tibetan Plateau. *Journal of Structural Geology*, *27*(1), 101–117. https://doi.org/10.1016/j.jsg.2004.06.010

He, S., Li, R., Wang, C., Zhang, H., Ji, W., Yu, P., et al. (2011). Discovery of~ 4.0 Ga detrital zircons in the Changdu Block, North Qiangtang, Tibetan Plateau. *Chinese Science Bulletin*, *56*(7), 647–658. https://doi.org/10.1007/s11434-010-4320-z

Hou, Z. Q. (1993). Tectono-magmatic evolution of the Yidun island-arc and geodynamic setting of Kuroko-type sulfid deposits in Sanjiang region, SW China. *Resource Geology Special Issue*, *17*, 336–350.

Huang, M. H., Buick, I. S., & Hou, L. W. (2003). Tectonometamorphic evolution of the eastern Tibet plateau: Evidence from the central Songpan–Garzê orogenic belt, Western China. *Journal of Petrology*, *44*(2), 255–278. https://doi.org/10.1093/petrology/44.2.255

Ingersoll, R. V., Dickinson, W. R., Graham, S. A., Chan, M. A., & Archer, A. W. (2003). Remnant-ocean submarine fans: Largest sedimentary systems on Earth. *Special Papers-Geological Society of America*, *370*, 191–208.

Jackson, W. T. Jr., Robinson, D. M., Weislogel, A. L., Jian, X., & McKay, M. P. (2018a). Cenozoic development of the nonmarine Mula basin in the Southern Yidun terrane: Deposition and deformation in the eastern Tibetan Plateau associated with the India-Asia collision. *Tectonics*, *37*, 2446–2465. https://doi.org/10.1029/2018TC004994

Jackson, W. T. Jr., Robinson, D. M., Weislogel, A. L., Shang, F., & Jian, X. (2018b). Mesozoic development of nonmarine basins in the northern Yidun terrane: Deposition and deformation in the eastern Tibetan Plateau prior to the India-Asia collision. *Tectonics*, *37*, 2466–2485. https://doi.org/10.1029/2018TC004995

Jian, X., Guan, P., Zhang, D. W., Zhang, W., Feng, F., Liu, R. J., & Lin, S. D. (2013). Provenance of Tertiary sandstone in the northern Qaidam basin, northeastern Tibetan Plateau: Integration of framework petrography, heavy mineral analysis and mineral chemistry. *Sedimentary Geology*, *290*, 109–125. https://doi.org/10.1016/j.sedgeo.2013.03.010

Jolivet, M., Brunel, M., Seward, D., Xu, Z., Yang, J., Roger, F., Tapponnier, P., et al. (2001). Mesozoic and Cenozoic tectonics of the northern edge of the Tibetan plateau: Fission-track constraints. *Tectonophysics*, *343*(1–2), 111–134. https://doi.org/10.1016/S0040-1951(01)00196-2

Kapp, P., Yin, A., Manning, C. E., Harrison, T. M., Taylor, M. H., & Ding, L. (2003). Tectonic evolution of the early Mesozoic blueschist-bearing Qiangtang metamorphic belt, central Tibet. *Tectonics*, *22*(4), 1043. https://doi.org/10.1029/2002TC001383

Kapp, P., Yin, A., Manning, C. E., Murphy, M., Harrison, T. M., Spurlin, M., et al. (2000). Blueschist-bearing metamorphic core complexes in the Qiangtang block reveal deep crustal structure of northern Tibet. *Geology*, *28*(1), 19–22. https://doi.org/10.1130/0091-7613(2000)28<19:BMCCIT>2.0.CO;2

Lease, R. O., Burbank, D. W., Gehrels, G. E., Wang, Z., & Yuan, D. (2007). Signatures of mountain building: Detrital zircon U/Pb ages from northeastern Tibet. *Geology*, *35*(3), 239–242. https://doi.org/10.1130/G23057A.1

Li, L., Meng, Q., Pullen, A., Garzione, C. N., Wu, G., Wang, Y., et al. (2014). Late Permian–early Middle Triassic back-arc basin development in West Qinling, China. *Journal of Asian Earth Sciences*, *87*, 116–129. https://doi.org/10.1016/j.jseaes.2014.02.021

Li, W., Neubauer, F., Liu, Y., Genser, J., Ren, S., Han, G., & Liang, C. (2013). Paleozoic evolution of the Qimantagh magmatic arcs, Eastern Kunlun Mountains: Constraints from zircon dating of granitoids and modern river sands. *Journal of Asian Earth Sciences*, *77*, 183–202. https://doi.org/10.1016/j.jseaes.2013.08.030

Li, X. H., Wang, C. S., Liu, S. G., Ran, B., Xu, W. L., & Zhou, Y. (2016). Chronology of the volcanic rock intercalations within the flysch of the Songpan-Ganzi folded belt and its geological significance (in Chinese with English Abstract). *Geological Bulletin of China*, *35*(6), 879–886.

Ling, W. L., Duan, R. C., Liu, X. M., Cheng, J. P., Mao, X. W., Peng, L. H., et al. (2010). U–Pb dating of detrital zircons from the Wudangshan Group in the South Qinling and its geological significance. *Chinese Science Bulletin*, *55*(22), 2440–2448. https://doi.org/10.1007/s11434-010-3095-6

Liu, S., Qian, T., Li, W., Dou, G., & Wu, P. (2015). Oblique closure of the northeastern Paleo-Tethys in central China. *Tectonics*, *34*, 413–434. https://doi.org/10.1002/2014TC003784

Liu, X. M., Gao, S., Diwu, C. R., & Ling, W. L. (2008). Precambrian crustal growth of Yangtze craton as revealed by detrital zircon studies. *American Journal of Science*, *308*(4), 421–468. https://doi.org/10.2475/04.2008.02

Liu, Y., Genser, J., Neubauer, F., Jin, W., Ge, X., Handler, R., & Takasu, A. (2005). 40Ar/39Ar mineral ages from basement rocks in the eastern Kunlun Mountains, NW China, and their tectonic implications. *Tectonophysics*, *398*(3–4), 199–224. https://doi.org/10.1016/j.tecto.2005.02.007

Lu, L., Zhang, K. J., Yan, L. L., Jin, X., & Zhang, Y. X. (2017). Was Late Triassic Tanggula granitoid (central Tibet, western China) a product of melting of underthrust Songpan-Ganzi flysch sediments? *Tectonics*, *36*, 902–928. https://doi.org/10.1002/2016TC004384

Ludwig, K. R. (2012). A geochronological toolkit for Microsoft Excel. *Berkeley Geochronology Center Special Publication*, *5*, 75.

Luo, L., Qi, J. F., Zhang, M. Z., Wang, K., & Han, Y. Z. (2014). Detrital zircon U–Pb ages of Late Triassic–Late Jurassic deposits in the western and northern Sichuan Basin margin: Constraints on the foreland basin provenance and tectonic implications. *International Journal of Earth Sciences*, *103*(6), 1553–1568. https://doi.org/10.1007/s00531-014-1032-7

Matte, P., Tapponnier, P., Arnaud, N., Bourjot, L., Avouac, J. P., Vidal, P., et al. (1996). Tectonics of Western Tibet, between the Tarim and the Indus. *Earth and Planetary Science Letters*, *142*(3–4), 311–330. https://doi.org/10.1016/0012-821X(96)00086-6

Meng, Q., Qu, H., & Hu, J. (2007). Triassic deep-marine sedimentation in the western Qinling and Songpan terrane. *Science in China Series D: Earth Sciences*, *50*(S2), 246–263. https://doi.org/10.1007/s11430-007-6009-y

Meng, Q. R., Wang, E., & Hu, J. M. (2005). Mesozoic sedimentary evolution of the northwest Sichuan basin: Implication for continued clockwise rotation of the South China block. *Geological Society of America Bulletin*, *117*(3), 396–410. https://doi.org/10.1130/B25407.1

Meng, Q. R., & Zhang, G. W. (2000). Geologic framework and tectonic evolution of the Qinling orogen, central China. *Tectonophysics*, *323*(3–4), 183–196. https://doi.org/10.1016/S0040-1951(00)00106-2

Metcalfe, I. (2006). Palaeozoic and Mesozoic tectonic evolution and palaeogeography of East Asian crustal fragments: The Korean Peninsula in context. *Gondwana Research*, *9*(1–2), 24–46. https://doi.org/10.1016/j.gr.2005.04.002

Mock, C., Arnaud, N. O., & Cantagrel, J. M. (1999). An early unroofing in northeastern Tibet? Constraints from 40Ar/39Ar thermochronology on granitoids from the eastern Kunlun Range (Qianghai, NW China). *Earth and Planetary Science Letters*, *171*(1), 107–122. https://doi.org/10.1016/S0012-821X(99)00133-8

Nie, S. Y., Yin, A., Rowley, D. B., & Jin, Y. G. (1994). Exhumation of the Dabie–Shan ultrahigh pressure rocks and accumulation of the Songpan-Ganzi flysch sequence, central China. *Geology*, *22*(11), 999–1002. https://doi.org/10.1130/0091-7613(1994)022<0999:EOTDSU>2.3.CO;2

Peng, T., Zhao, G., Fan, W., Peng, B., & Mao, Y. (2014). Zircon geochronology and Hf isotopes of Mesozoic intrusive rocks from the Yidun terrane, Eastern Tibetan Plateau: Petrogenesis and their bearings with Cu mineralization. *Journal of Asian Earth Sciences*, *80*, 18–33. https://doi.org/10.1016/j.jseaes.2013.10.028

Pullen, A., & Kapp, P. (2014). Mesozoic tectonic history and lithospheric structure of the Qiangtang terrane: Insights from the Qiangtang metamorphic belt, central Tibet. *Geological Society of America Special Papers*, *507*, 71–87. https://doi.org/10.1130/2014.2507(04)

Pullen, A., Kapp, P., Gehrels, G. E., Vervort, J. D., & Ding, L. (2008). Triassic continental subduction in central Tibet and Mediterranean-style closure of the Paleo-Tethys Ocean. *Geology*, *36*(5), 5351–5354. https://doi.org/10.1130/G24435A.1

Ratschbacher, L., Hacker, B. R., Calvert, A., Webb, L. E., Grimmer, J. C., McWilliams, M. O., et al. (2003). Tectonics of the Qinling (Central China): Tectonostratigraphy, geochronology, and deformation history. *Tectonophysics*, *366*(1–2), 1–53. https://doi.org/10.1016/S0040-1951(03)00053-2

Reid, A., Wilson, C. J. L., Shun, L., Pearson, N., & Belousova, E. (2007). Mesozoic plutons of the Yidun Arc, SW China: U/Pb geochronology and Hf isotopic signature. *Ore Geology Reviews*, *31*(1–4), 88–106. https://doi.org/10.1016/j.oregeorev.2004.11.003

Reid, A. J., Wilson, C. J. L., & Liu, S. (2005). Structural evidence for the Permo–Triassic tectonic evolution of the Yidun Arc, eastern Tibetan Plateau. *Journal of Structural Geology*, *27*(1), 119–137. https://doi.org/10.1016/j.jsg.2004.06.011

Roger, F., Arnaud, N., Gilder, S., Tapponnier, P., Jolivet, M., Brunel, M., et al. (2003). Geochronological and geochemical constraints on Mesozoic suturing in east central Tibet. *Tectonics*, *22*(4), 1037. https://doi.org/10.1029/2002TC001466

Roger, F., Jolivet, M., & Malavieille, J. (2010). The tectonic evolution of the Songpan-Garzê (North Tibet) and adjacent areas from Proterozoic to Present: A synthesis. *Journal of Asian Earth Sciences*, *39*(4), 254–269. https://doi.org/10.1016/j.jseaes.2010.03.008

Roger, F., Malavieille, J., Leloup, P. H., Calassou, S., & Xu, Z. (2004). Timing of granite emplacement and cooling in the Songpan-Garze fold belt (eastern Tibetan Plateau) with tectonic implications. *Journal of Asian Earth Sciences*, *22*(5), 465–481. https://doi.org/10.1016/S1367-9120(03)00089-0

Royden, L. J., Burchfiel, B. C., King, R. W., Wang, E., Chen, Z., Shen, F., & Liu, Y. (1997). Surface deformation and lower crustal flow in eastern Tibet. *Science*, *276*(5313), 788–790. https://doi.org/10.1126/science.276.5313.788

Shang, F. (2016). *Mesozoic History of the southeastern Tibetan Plateau: Sediment provenance, paleoclimate, and surface elevation History, (doctoral dissertation)*. Retrieved from ProQuest Dissertations Publishing, 2016.10110103. Morgantown, WV: West Virginia University.

She, Z., Ma, C., Mason, R., Li, J., Wang, G., & Lei, Y. (2006). Provenance of the Triassic Songpan–Ganzi flysch, west China. *Chemical Geology*, *231*(1–2), 159–175. https://doi.org/10.1016/j.chemgeo.2006.01.001

Song, X. Y., Zhou, M. F., Cao, Z. M., & Robinson, P. T. (2004). Late Permian rifting of the South China Craton caused by the Emeishan mantle plume? *Journal of the Geological Society*, *161*(5), 773–781. https://doi.org/10.1144/0016-764903-135

Tung, K. A., Yang, H. J., Yang, H. Y., & Liu, D. Y. (2007). SHRIMP U–Pb geochronology of the zircons from the Precambrian basement of the Qilian Block and its geological significances. *Chinese Science Bulletin*, *52*(19), 2687–2701. https://doi.org/10.1007/s11434-007-0356-0

Tung, K. A., Yang, H. Y., Liu, D. Y., Zhang, J. X., Tseng, C. Y., & Wan, Y. S. (2007). SHRIMP U–Pb geochronology of the detrital zircons from the Longshoushan Group and its tectonic significance. *Chinese Science Bulletin*, *52*(10), 1414–1425. https://doi.org/10.1007/s11434-007-0189-x

Uddin, A., & Lundberg, N. (1998). Cenozoic history of the Himalayan-Bengal system: Sand composition in the Bengal basin, Bangladesh. *Geological Society of America Bulletin*, *110*(4), 497–511. https://doi.org/10.1130/0016-7606(1998)110<0497:CHOTHB>2.3.CO;2

Vermeesch, P. (2012). On the visualization of detrital age distributions. *Chemical Geology*, *312–313*, 190–194. https://doi.org/10.1016/j.chemgeo.2012.04.021

Wan, Y. S., Liu, D. Y., Dong, C. Y., & Yin, X. Y. (2011). SHRIMP zircon dating of metasedimentary rock from the Qinling Group in the north of Xixia, North Qinling Orogenic Belt: Constraints on complex histories of source region and timing of deposition and metamorphism. *Acta Petrologica Sinica*, *27*, 1172–1178.

Wang, B. Q., Wang, W., Chen, W. T., Gao, J. F., Zhao, X. F., Yan, D. P., & Zhou, M. F. (2013). Constraints of detrital zircon U–Pb ages and Hf isotopes on the provenance of the Triassic Yidun Group and tectonic evolution of the Yidun terrane, eastern Tibet. *Sedimentary Geology*, *289*, 74–98. https://doi.org/10.1016/j.sedgeo.2013.02.005

Wang, B. Q., Zhou, M. F., Chen, W. T., Gao, J. F., & Yan, D. P. (2013). Petrogenesis and tectonic implications of the Triassic volcanic rocks in the northern Yidun terrane, eastern Tibet. *Lithos*, *175–176*, 285–301. https://doi.org/10.1016/j.lithos.2013.05.013

Wang, L. J., Griffin, W. L., Yu, J. H., & O'Reilly, S. Y. (2010). Precambrian crustal evolution of the Yangtze Block tracked by detrital zircons from Neoproterozoic sedimentary rocks. *Precambrian Research*, *177*(1–2), 131–144. https://doi.org/10.1016/j.precamres.2009.11.008

Wang, Q., Li, Z. X., Chung, S. L., Wyman, D. A., Sun, Y. L., Zhao, Z. H., Zhu, Y. T., et al. (2011). Late Triassic high-Mg andesite/dacite suites from northern HohXil, North Tibet: Geochronology, geochemical characteristics, petrogenetic processes and tectonic implications. *Lithos*, *126*(1–2), 54–67. https://doi.org/10.1016/j.lithos.2011.06.002

Weislogel, A. L. (2008). Tectonostatigraphic and geochronologic constraints on evolution of the northeast Paleotethys from the Songpan-Ganzi Complex, central China. *Tectonophysics*, *451*(1–4), 331–345. https://doi.org/10.1016/j.tecto.2007.11.053

Weislogel, A. L., Graham, S. A., Chang, E. Z., Wooden, J. L., & Gehrels, G. E. (2010). Detrital zircon provenance from three turbidite depocenters of the Middle-Upper Triassic Songpan–Ganzi complex, central China: Record of collisional tectonics, erosional exhumation, and sediment production. *Geological Society of America Bulletin*, *122*(11–12), 2041–2062. https://doi.org/10.1130/B26606.1

Weislogel, A. L., Graham, S. A., Chang, E. Z., Wooden, J. L., Gehrels, G. E., & Yang, H. (2006). Detrital zircon provenance of the Late Triassic Songpan-Ganzi Complex: Sedimentary record of collision of the North and South China blocks. *Geology*, *34*(2), 97–100. https://doi.org/10.1130/G21929.1

Wilde, S., Zhao, G., & Sun, M. (2002). Development of the North China Craton during the late Archaean and its final amalgamation at 1.8 Ga: Some speculations on its position within a global Palaeoproterozoic supercontinent. *Gondwana Research*, *5*(1), 85–94. https://doi.org/10.1016/S1342-937X(05)70892-3

Worley, B. A., & Wilson, C. J. (1996). Deformation partitioning and foliation reactivation during transpressional orogenesis, an example from the Central Longmen Shan, China. *Journal of Structural Geology*, *18*(4), 395–411. https://doi.org/10.1016/0191-8141(95)00095-U

Wu, T., Xiao, L., Wilde, S. A., Ma, C. Q., Li, Z. L., Sun, Y., & Zhan, Q. Y. (2016). Zircon U-Pb age and Sr-Nd-Hf isotope geochemistry of the Ganluogou dioritic complex in the northern Triassic Yidun arc belt, Eastern Tibetan Plateau: Implications for the closure of the Garzê-Litang Ocean. *Lithos*, *248–251*, 94–108. https://doi.org/10.1016/j.lithos.2015.12.029

Xia, X. P., Sun, M., Zhao, G. C., & Luo, Y. (2006). LA-ICP-MS U–Pb geochronology of detrital zircons from the Jining Complex, North China Craton and its tectonic significance. *Precambrian Research*, *144*(3–4), 199–212. https://doi.org/10.1016/j.precamres.2005.11.004

Xu, Z., Hou, L., & Wang, Z. (1992). *Orogenic Process of the Songpan–Garze Orogenic Belt of China* (in Chinese with English abstract) (pp. 1–190). Beijing: Geological Publishing House.

Yan, Z., Aitchison, J., Fu, C., Guo, X., Niu, M., Xia, W., & Li, J. (2015). Hualong Complex, South Qilian terrane: U–Pb and Lu–Hf constraints on Neoproterozoic micro-continental fragments accreted to the northern Proto-Tethyan margin. *Precambrian Research*, *266*, 65–85. https://doi.org/10.1016/j.precamres.2015.05.001

Yan, Z., Guo, X., Fu, C., Aitchison, J., Wang, Z., & Li, J. (2014). Detrital heavy mineral constraints on the Triassic tectonic evolution of the West Qinling terrane, NW China: Implications for understanding subduction of the Paleotethyan Ocean. *The Journal of Geology*, *122*(5), 591–608. https://doi.org/10.1086/677264

Yang, J. S., Robinson, P. T., Jiang, C. F., & Xu, Z. Q. (1996). Ophiolites of the Kunlun Mountains, China and their tectonic implications. *Tectonophysics*, *258*(1–4), 215–231. https://doi.org/10.1016/0040-1951(95)00199-9

Yang, T. N., Ding, Y., Zhang, H. R., Fan, J. W., Liang, M. J., & Wang, X. H. (2014). Two-phase subduction and subsequent collision defines the Paleotethyan tectonics of the southeastern Tibetan Plateau: Evidence from zircon U-Pb dating, geochemistry, and structural geology of the Sanjiang orogenic belt, southwest China. *Bulletin*, *126*(11–12), 1654–1682. https://doi.org/10.1130/B30921.1

Yang, T. N., Hou, Z. Q., Wang, Y., Zhang, H. R., & Wang, Z. L. (2012). Late Paleozoic to Early Mesozoic tectonic evolution of northeast Tibet: Evidence from the Triassic composite western Jinsha-Garzê-Litang suture. *Tectonics*, *31*, TC4004. https://doi.org/10.1029/2011TC003044

Yin, A., & Harrison, T. M. (2000). Geologic evolution of the Himalayan–Tibetan orogen. *Annual Review of Earth and Planetary Sciences*, *28*(1), 211–280. https://doi.org/10.1146/annurev.earth.28.1.211

Yin, A., & Nie, S. (1993). An indentation model for the North and South China collision and the development of the Tan-Lu and Honam fault systems, eastern Asia. *Tectonics*, *12*, 801–813. https://doi.org/10.1029/93TC00313

Yin, A., & Nie, S. Y. (1996). *A phanerozoic palinspastic reconstruction of China and its neighboring regions*, *World and Regional Geology* (pp. 442–485). New York: Cambridge University Press.

Yin, H. F., Yang, F. Q., Huang, Q. S., Yang, H. S., & Lai, X. L. (1992). *The Triassic of Qinling Mountains* (in Chinese with English abstract). Wuhan: China University of Geosciences Press.

Yong, L., Allen, P. A., Densmore, A. L., & Qiang, X. (2003). Evolution of the Longmen Shan foreland basin (western Sichuan, China) during the Late Triassic Indosinian orogeny. *Basin Research*, *15*(1), 117–138. https://doi.org/10.1046/j.1365-2117.2003.00197.x

Yuan, C., Zhou, M. F., Sun, M., Zhao, Y., Wilde, S., Long, X., & Yan, D. (2010). Triassic granitoids in the eastern Songpan Ganzi Fold Belt, SW China: Magmatic response to geodynamics of the deep lithosphere. *Earth and Planetary Science Letters*, *290*(3–4), 481–492. https://doi.org/10.1016/j.epsl.2010.01.005

Zhang, K. J., Li, B., Wei, Q. G., Cai, J. X., & Zhang, Y. X. (2008). Proximal provenance of the western Songpan–Ganzi turbidite complex (Late Triassic, eastern Tibetan plateau): Implications for the tectonic amalgamation of China. *Sedimentary Geology*, *208*(1–2), 36–44. https://doi.org/10.1016/j.sedgeo.2008.04.008

Zhang, K. J., Zhang, Y. X., Li, B., Zhu, Y. T., & Wei, R. Z. (2006). The blueschist-bearing Qiangtang metamorphic belt (northern Tibet, China) as an in situ suture zone: Evidence from geochemical comparison with the Jinsa suture. *Geology*, *34*(6), 493–496. https://doi.org/10.1130/G22404.1

Zhang, L. Y., Ding, L., Pullen, A., Xu, Q., Liu, D. L., Cai, F. L., et al. (2014). Age and geochemistry of western Hoh-Xil–Songpan-Ganzi granitoids, northern Tibet: Implications for the Mesozoic closure of the Paleo-Tethys ocean. *Lithos*, *190–191*, 328–348. https://doi.org/10.1016/j.lithos.2013.12.019

Zhang, Y. X., Tang, X. C., Zhang, K. J., Zeng, L., & Gao, C. L. (2014). U–Pb and Lu–Hf isotope systematics of detrital zircons from the Songpan–Ganzi Triassic flysch, NE Tibetan Plateau: Implications for provenance and crustal growth. *International Geology Review*, *56*(1), 29–56. https://doi.org/10.1080/00206814.2013.818754

Zhou, D., & Graham, S. A. (1996). The Songpan-Ganzi Complex of the West Qinling Shan as a Triassic remnant ocean basin. In A. Yin & T. M. Harrison (Eds.), *Tectonic Evolution of Asia* (pp. 281–299). Cambridge: Cambridge University Press.

Zhu, X. Y., Chen, F. K., Li, S. Q., Yang, Y. Z., Nie, H., Siebel, W., & Zhai, M. G. (2011). Crustal evolution of the North Qinling terrain of the Qinling Orogen, China: Evidence from detrital zircon U–Pb ages and Hf isotopic composition. *Gondwana Research*, *20*(1), 194–204. https://doi.org/10.1016/j.gr.2010.12.009

Zi, J. W., Cawood, P. A., Fan, W. M., Wang, Y. J., & Tohver, E. (2012). Contrasting rift and subduction-related plagiogranites in the Jinshajiang ophiolitic mélange, Southwest China, and implications for the Paleo-Tethys. *Tectonics*, *31*, TC2012. https://doi.org/10.1029/2011TC002937